RESEARCH ARTICLE

Monoterpenes Support Systemic Acquired Resistance Within and Between Plants

Marlies Riedlmeier[1,§], Andrea Ghirardo[2,§], Marion Wenig[1,§], Claudia Knappe[1], Kerstin Koch[2], Elisabeth Georgii[1], Sanjukta Dey[1], Jane E. Parker[3], Jörg-Peter Schnitzler[2], and A. Corina Vlot[1,*]

[1]Helmholtz Zentrum Muenchen, Department of Environmental Sciences, Institute of Biochemical Plant Pathology, D-85764 Neuherberg, Germany; [2]Helmholtz Zentrum Muenchen, Institute of Biochemical Plant Pathology, Research Unit Environmental Simulation, D-85764 Neuherberg, Germany; [3]Max Planck Institute for Plant Breeding Research, Department of Plant-Microbe Interactions, D-50829 Cologne, Germany
[§]These authors contributed equally to this work
*Corresponding author: A. Corina Vlot
Tel: +49-89-31873985
E-Mail: corina.vlot@helmholtz-muenchen.de

Short title: Volatile signals in innate immunity

One-sentence summary: Infection of *Arabidopsis thaliana* with avirulent *Pseudomonas syringae* induces camphene and α- and β-pinene emissions contributing to systemic resistance induction in the same and neighboring plants.

The author responsible for distribution of materials integral to the findings presented in this article in accordance with the policy described in the Instructions for Authors (www.plantcell.org) is: A. Corina Vlot (corina.vlot@helmholtz-muenchen.de).

Abstract
This study investigates the role of volatile organic compounds in systemic acquired resistance (SAR), a salicylic acid (SA)-associated, broad-spectrum immune response in systemic, healthy tissues of locally infected plants. Gas chromatography coupled to mass spectrometry analyses of SAR-related emissions of wild-type and non-SAR-signal-producing mutant plants associated SAR with monoterpene emissions. Headspace exposure of *Arabidopsis thaliana* to a mixture of the bicyclic monoterpenes α-pinene and β-pinene induced defense, accumulation of reactive oxygen species, and expression of SA- and SAR-related genes, including the SAR regulatory *AZELAIC ACID INDUCED1* (*AZI1*) gene and three of its paralogs. Pinene-induced resistance was dependent on SA biosynthesis and signaling and on *AZI1*. *A. thaliana geranylgeranyl reductase1* mutants with reduced monoterpene biosynthesis were SAR-defective but mounted normal local resistance and methyl salicylate-induced defense responses, suggesting that monoterpenes act in parallel with SA. The volatile emissions from SAR signal-emitting plants induced defense in neighboring plants and this was associated with the presence of α-pinene, β-pinene, and camphene in the emissions of the 'sender' plants. Our data suggest that monoterpenes, particularly pinenes, promote SAR, acting through ROS and *AZI1*, and likely function as infochemicals in plant-to-plant signaling, thus allowing defense signal propagation between neighboring plants.

Introduction

As sessile organisms, plants are equipped with a sophisticated multi-layered immune system including constitutive and inducible defenses (Spoel and Dong, 2012). Non-host resistance is the most robust and durable form of plant resistance to the majority of non-adapted microbes. If a host-adapted pathogen penetrates constitutive barriers of the plant's surface and cell wall, it encounters the extracellular space where, for example, pattern recognition receptors (PRRs) can recognize conserved microbial structures (elicitors, pathogen-associated molecular patterns, PAMPs) (Macho and Zipfel, 2014). PRRs are located in the plasma membrane and contain an extracellular ligand recognition domain, often fused to an intracellular kinase signaling domain. Activation of PRRs induces a battery of host responses, including stomatal closure, a burst of reactive oxygen species (ROS), mitogen-activated protein kinase activation, salicylic acid (SA) production, and changes in host gene expression, known collectively as PAMP-triggered immunity (PTI) (Jones and Dangl, 2006; Spoel and Dong, 2012; Macho and Zipfel, 2014). Driven by natural selection, host-adapted pathogens have evolved effectors, many of which are secreted into the host cytoplasm to suppress PTI, resulting in effector-triggered susceptibility (ETS) (Jones and Dangl, 2006). ETS, in turn, can be counteracted by plant RESISTANCE (R) proteins that recognize specific pathogen effectors and induce effector-triggered immunity (ETI) (Jones and Dangl, 2006; Spoel and Dong, 2012; Cui et al., 2015). Compared to PTI, ETI is generally a more robust form of plant defense, often culminating in a local hypersensitive response (HR) involving programmed cell death (PCD), which isolates the pathogen and protects remaining plant tissues from infection (Cui et al, 2015; Mur et al., 2008).

Both PTI and ETI trigger SA accumulation and expression of the SA marker gene *PATHOGENESIS-RELATED1* (*PR1)* in infected and also distal uninfected tissues of locally infected plants. The latter reaction is part of an inducible defense response known as systemic acquired resistance (SAR), a long-lasting SA-dependent immunity against a broad spectrum of (hemi-)biotrophic pathogens (Spoel and Dong, 2012; Fu and Dong, 2013; Shah et al., 2014). Putative long-distance signals that move from infected to distal tissues to induce SAR include the volatile methylated derivative of SA (methyl salicylate, MeSA; Park et al., 2007), the dicarboxylic acid azelaic acid (AzA; Jung et al., 2009), the abietane diterpenoid dehydroabietinal (DA; Chaturvedi

et al., 2012), a glycerol-3-phosphate (G3P)-derivative (Chanda et al., 2011), the predicted lipid transfer proteins DEFECTIVE IN INDUCED RESISTANCE1 (DIR1) and DIR1-like (Maldonado et al., 2002; Champigny et al., 2013), and the non-protein amino acid pipecolic acid (Navarova et al., 2012). Most of these molecules are believed to act in parallel with SA in systemic but not local resistance responses. SAR-modulating interactions between these signals are increasingly recognized (Dempsey and Klessig, 2012; Shah et al., 2014; Gao et al., 2015). AzA, for example, appears to act synergistically with DA (Chaturvedi et al., 2012) and upstream of G3P, which promotes SAR in a positive feedback loop with DIR1 and AZELAIC ACID INDUCED 1 (AZI1), possibly together with DIR1-like and one or more paralogs of AZI1, including EARLY *ARABIDOPSIS* ALUMINIUM INDUCED1 (EARLI1) (Yu et al., 2013; Cecchini et al., 2015; Gao et al., 2015).

ENHANCED DISEASE SUSCEPTIBILITY1 (EDS1) is a nucleocytoplasmic, lipase-like protein that promotes the transcriptional reprogramming of parallel SA-dependent and SA-independent defense signaling pathways (Feys et al., 2001; Bartsch et al., 2006; Garcia et al, 2010; Cui et al., 2017) in basal immunity against virulent pathogens and ETI conferred by intracellular nucleotide-binding/leucine rich repeat (NB-NLR) receptors (Aarts et al., 1998; Vlot et al., 2009; Cui et al., 2017). To mobilize these pathways, EDS1 forms heteromeric complexes with either one of its sequence-related partners, PHYTOALEXIN-DEFICIENT4 (PAD4) or SENESCENCE ASSOCIATED GENE101 (SAG101) (Feys et al., 2001, 2005, Vlot et al., 2009, Rietz et al., 2011, Wagner et al., 2013). EDS1 nuclear accumulation is essential for transcriptional defense reprogramming in basal immunity and ETI mediated by a major sub-class of NB-LRR receptors called TIR-NB-LRRs (possessing a Toll-Interleukin1-receptor-like (TIR) N-terminal domain) (Garcia et al., 2010; Bhattacharjee et al., 2011; Heidrich et al., 2011; Stuttmann et al., 2016).

During SAR, EDS1 is required both for generating the SAR signal in primary infected leaves and for perceiving the SAR signal in systemic uninfected tissues (Breitenbach et al., 2014). In *Arabidopsis thaliana*, pathogen infection with *Pseudomonas syringae* carrying the effector *AvrRpm1* activates ETI via the coiled-coil NB-LRR (CC-NB-LRR) receptor RESISTANCE TO PSEUDOMONAS SYRINGAE pathovar MACULICOLA1 (RPM1) (Dangl et al., 1992). Although RPM1-triggered local SA-dependent immune responses and PCD genetically do not require *EDS1* (Aarts et al., 1998), both *eds1*

and *pad4* mutant plants are SAR-defective after local RPM1 activation (Truman et al., 2007, Jing et al., 2011; Rietz et al., 2011; Breitenbach et al., 2014).

Previously, we exploited the SAR-specific phenotype of the *eds1* mutant in response to conditionally expressed *AvrRpm1* to identify proteins and metabolites that are associated with SAR (Breitenbach et al., 2014, Wittek et al., 2014, 2015). Here, we identify SAR-associated volatile organic compounds (VOCs) that are emitted from *A. thaliana* rosettes in an *EDS1*-dependent manner in response to *AvrRpm1.* So far, VOCs in plant defense have been implicated mostly in direct and indirect responses to herbivory (Dicke, 2009; Ghirardo et al., 2012; Scala et al., 2013a; Pierik et al., 2014; Dong et al., 2016). However, there are indications that plant-, bacteria-, or fungus-derived VOCs can affect plant innate immunity (Yi et al., 2009; Dicke and Baldwin, 2010; Scala et al., 2013a, 2013b; Choi et al., 2014; Naznin et al., 2014; Song et al., 2015). Also, in addition to the putative role of the volatile benzenoid MeSA in SAR, further possible functions of VOCs in SAR have been discussed (Heil and Ton, 2008) but have remained largely uninvestigated to date.

In this study, we present the first comprehensive analysis of *A. thaliana* VOC emissions during SAR signaling. Using gas chromatography coupled to mass spectrometry (GC-MS), plant head space exposure, and transcript profiling approaches as well as *A. thaliana* mutants, we found that monoterpenoid VOCs are highly correlated with SAR competence. We further established that monoterpenes play an essential role in plant-to-plant innate immune signaling, suggesting that monoterpenoid VOCs are part of an ecologically relevant mechanism to relay signals to other plants in the nearby environment.

Results

Identification of SAR-related VOCs

SAR signaling was induced by dexamethasone (DEX) treatment of four- to five-week-old transgenic plants expressing haemagglutinin (HA)-tagged *AvrRpm1* from a DEX-inducible transgene (*pDEX:AvrRpm1-HA*) in the Col-0 wild type (wt) and *eds1-2* genetic backgrounds of *A. thaliana* (Breitenbach et al., 2014). Significant VOC emissions were observed 1–7 h after the onset of the treatment. VOCs were collected during two sampling periods (SPs): between 1 and 4 h (SP1) and 4 and 7 h

(SP2) after the DEX treatment. Using GC-MS, we detected a total of 39 compounds in background-corrected emission profiles from DEX-treated Col-0 *DEX:AvrRpm1-HA* and *eds1-2 DEX:AvrRpm1-HA* plants. Chemical identification indicated the presence of 5 mono- and 3 sesquiterpenes, while the remaining compounds were classified as fatty esters, fatty aldehydes, alkanes, aromatics, and alcohols (Supplemental Table 1).

Multivariate data analysis (MDA) of the VOC emission rates from DEX-treated Col-0 *DEX:AvrRpm1-HA* and *eds1-2 DEX:AvrRpm1-HA* plants revealed a clear separation of Col-0 and *eds1-2* profiles during both sampling periods (SP1: Figure 1 A and SP2: Figure 1 B). Partial least square regression (PLSR) using the regression type OPLS (orthogonal PLS) of samples collected during SP1 (Figure 1 A, C, and E) indicated that ß-pinene, α-pinene, camphene, isopropyl palmitate, and sabinene were the strongest discriminant compounds between Col-0- and *eds-1-2*-derived samples ($P=0.012$; CV-ANOVA) and were emitted at statistically different emission rates ($P<0.01$, Student's *t*-test) (marked in red in Figure 1 C and E; see also Supplemental Table 1). The same analysis of samples collected during SP2 (Figure 1 B, D, and F) confirmed that release of these VOCs was significantly different ($P<0.05$, CV-ANOVA) between the two genotypes, although to a lesser extent compared to SP1. Overall, five VOCs were negatively correlated with *eds1-2* in samples collected during SP1 (Figure 1 E), and the emissions of α-pinene, ß-pinene, and camphene (Figure 2 A) were not detected from DEX-treated *eds1-2 DEX:AvrRpm1-HA* plants during both sampling periods (Figure 2 B–D). Emissions of the monoterpene sabinene and of isopropyl palmitate, the ester of isopropylalcohol and palmitic acid (C_{19}), were reduced in *eds1-2* compared to wt plants, but remained detectable (Figure 2 E–F). In DEX-treated Col-0 *DEX:AvrRpm1-HA* plants, the monoterpene emissions tended to decrease from the early time point, SP1, to the later one, SP2, indicating that the weaker difference between Col-0 and *eds1-2* seen with MDA in SP2 was due to an overall decrease in emission rates.

Together, the data associate the SAR deficiency of *eds1* mutant plants with reduced emissions of at least five VOCs. Notably, four of these compounds are closely related monoterpenes: α-pinene, ß-pinene, camphene (Figure 2 A) and sabinene are biochemically produced from the same plastidic isoprenoid pathway (Tholl and Lee, 2011). Almost undetectable emissions of α-pinene, ß-pinene, and camphene from

eds1-2 mutant plants (Figure 2 B-D) prompted us to investigate whether these monoterpenes have a role in inducing SAR.

Monoterpenes enhance *A. thaliana* resistance to *P. syringae* bacteria

To assess the possible biological relevance of α-pinene, ß-pinene, and camphene in plant immunity, an experimental set-up was designed to treat plants with individual compounds in gas-tight glass desiccators. In these 5.5 liter compartments, eight 4.5-week-old *A. thaliana* wt Col-0 plants were incubated over 3 days (d) with different amounts of either camphene or a mixture of the structural isomers α- and β-pinene 1:1 (v:v) (Pin). The pinene mixture contained both of the α-pinene enantiomers ((±)-α-pinene) and the naturally prevalent β-pinene enantiomer (-)-β-pinene (Figure 2 A). Different monoterpenes, MeSA as a positive control, or the VOC solvent hexane as a negative control, were applied onto a filter paper in the desiccators. Every 24 h, the supplemented air was replaced with fresh air from the inflow of the growth chamber. After changing the air, the appropriate monoterpene, or the MeSA or hexane treatments, were applied again. After 3 d, plants were removed from the desiccators and two fully expanded leaves were inoculated with *P. syringae* pv *tomato* strain DC3000 (*Pst*). *Pst* bacterial growth was then monitored by measuring *in planta Pst* titers at four d post inoculation (dpi).

Park et al. (2007) showed that treatment of tobacco leaves with MeSA enhanced the systemic resistance of the plants to tobacco mosaic virus. Pre-experiments with different concentrations of MeSA revealed that *A. thaliana* required ~22-fold less MeSA for maximal defense induction compared to the concentrations applied to tobacco (Park et al., 2007). *A. thaliana* wt plants that had been exposed to 1.6 µmole MeSA for 3 d supported ~10-fold less growth of *Pst* compared to plants that had been exposed to the hexane solvent only (negative control), indicating that resistance to *Pst* was induced by MeSA (Figure 3 A), presumably due to its conversion to SA (Shulaev et al., 1997; Koo et al., 2007; Park et al., 2007). A similar reduction in *Pst* growth was observed after incubation of wt plants with the pinene mixture in a concentration-dependent manner, suggesting that α- and/or β-pinene enhanced *A. thaliana* resistance to *Pst* (Figure 3 A). Treatment of plants with 0.6 µmole of the pinene mixture, which amounts to a concentration in the headspace of ~2.6 ppmv (parts per million by volume), triggered the strongest defense response and was used

in all subsequent head space exposure experiments. We next assessed if and how the length of the headspace exposure affects pinene-induced resistance. Pilot experiments showed that the pinene mixture did not enhance resistance to *Pst* or *PR1* transcript accumulation in the treated plants if the 3-d exposure time was reduced to 1 d (see lane 6 in Figure 8 D) or 2 d, respectively. To exclude a possible effect of shorter pinene exposures if plants were left additional time to respond, we kept 1-d exposed plants in the growth chamber for 2 additional days (time point 1+2d) and 2-d exposed plants for 1 additional day (time point 2+1d) before inoculating them with *Pst*. Because *Pst* growth was significantly reduced after 3 d of headspace exposure to 0.6 µmole of the pinene mixture, but not after the 1+2d and 2+1d treatments (Figure 3 B), we concluded that the pinene mixture must be applied for three consecutive days to induce defense. Once established, the pinene-induced defense response was relatively stable, reducing growth of a *Pst* inoculum that was applied 1 or 3 d after the completion of a 3-d headspace exposure (Supplemental Figure 1; time points 3+1d and 3+3d).

Similarly to the emissions of α- and ß-pinene, camphene emissions from *AvrRpm1*-expressing *eds1-2* plants were reduced to levels below the detection limit (Figure 2 D). Also, headspace exposure of plants to camphene reduced *Pst* growth in leaves to a similar extent as the pinene mixture (Figure 3 C). Notably, camphene enhanced plant resistance to *Pst* when applied at a lower amount of 0.1 µmole, which amounted to a concentration in the headspace of ~0.4 ppmv. The application of higher camphene amounts (0.7 and 1.4 µmole, Figure 3 C) did not enhance *A. thaliana* resistance to *Pst* growth. This is comparable to our previous findings for SAR-inducing folates and the AzA precursor 9-oxo nonanoic acid, which trigger SAR in a concentration-dependent manner and lose their activity when applied at higher concentrations (Wittek et al., 2014, 2015). Together, the data suggest that SAR is sensitive to the concentration of (*EDS1*-dependent) SAR signaling components. Here, the resistance-inducing capacity of camphene was confirmed in combination with the pinene mixture. Exposing plants to 0.1 µmole of camphene and 0.6 µmole of the pinene mixture reduced *Pst* growth compared to each of the individual treatments (Figure 3 D), suggesting that camphene acts additively with α- and ß-pinene in the induction of defense.

Because monoterpenes are believed to have antimicrobial activity (Tholl and Lee, 2011), we excluded a possible toxic effect of the pinene mixture and of camphene on *Pst* by propagating serial dilutions of *Pst* on plates that were either supplemented with 500 µM of the VOCs or incubated in desiccators and exposed to the VOC amounts that enhanced plant resistance to *Pst* (Supplemental Figure 2). Neither of these treatments compromised *Pst* growth compared to that of the untreated controls or of *Pst* propagated in the presence of MeSA or the hexane solvent amount corresponding to that in the pinene mixture and camphene. Because camphene and both pinenes are thus likely non-toxic to *Pst*, the data suggest that these compounds act as infochemicals that promote *A. thaliana* resistance to *Pst* growth *in planta.*

In plants, both enantiomers of α-pinene, i.e., (+)-α-pinene and (-)-α-pinene, can co-occur, while β-pinene is generally found as the (-)-isoform (Finefield et al., 2012), which was included in the pinene mixture. Next, we sought to ascertain if (-)-β-pinene has an enantiomer-specific function in plant immunity. As shown above, the headspace exposure of plants with the pinene mixture reduced growth of subsequently applied *Pst* bacteria (Figure 3 E). A similar reduction in *Pst* growth was observed in plants that had been treated with a mixture of (±)-α-pinene and (+)-β-pinene compared to the hexane-treated plants (Figure 3 E), indicating that the bioactivity of β-pinene in *A. thaliana* immunity is not enantiomer-specific. By contrast, treatment of plants with either (±)-α-pinene or (-)-β-pinene alone did not reduce *Pst* growth compared to that in hexane-treated plants (Figure 3 F). Therefore, both α- and β-pinene appear to be required for pinene-induced immunity in *A. thaliana*.

Because commercially available natural compounds are often not sold as pure chemicals, it was crucial to analyze the purity of the VOC standards by GC-MS analysis. Camphene was relatively pure and did not contain additional monoterpene compounds (Supplemental Figure 3). By contrast, the purity of the (±)-α-pinene and (-)-β-pinene standards that were used over the course of the experiments ranged from relatively pure (Supplemental Figure 3 B) to contaminated with >10% of camphene and >5% of the monoterpene limonene (Supplemental Figure 3 A). The monocyclic monoterpene limonene had previously been associated with plant immunity (Rodríguez et al., 2014) and herein also enhanced *A. thaliana* resistance to *Pst* when applied in amounts ranging from 0.08 to 0.8 µmole (Supplemental Figure 4). Although 0.08 µmole of limonene approximately corresponded to the amount of

limonene present in the pinene mixture that was used in the experiments summarized in Figures 3 A and C, limonene-induced resistance was less robust than pinene-induced resistance, particularly in the lower concentration range, suggesting that limonene contamination was not (alone) causal for the observed pinene-induced resistance response. Also, later experiments with relatively pure compounds (Supplemental Figure 3 B) showed that a mixture of (±)α- and either (-) or (+)β-pinene sufficed to enhance plant resistance to *Pst* (Figures 3 B and D–F). In summary, headspace exposure of *A. thaliana* to the monoterpenes pinene and camphene (Figure 3) enhances plant immunity to *Pst* in a manner that is dependent on the concentration and, in the case of pinene, on the presence of both structural isomers of the compound in the volatile blend.

Monoterpene-induced resistance depends on SA and *AZI1*

In the following experiments, we analyzed the role of monoterpenes in *A. thaliana* immunity and their relation to SA. First, we investigated whether *EDS1* is necessary for the plant defense response to headspace exposure with pinenes, besides its role upstream of monoterpene emission (Figure 1 and 2). We also studied effects of volatile pinenes on the *non-expressor of PR genes1-1* (*npr1-1*) mutant, which is defective in signaling downstream of SA (Cao et al., 1997; Vlot et al., 2009). As expected, treatment of wt plants with either MeSA or the pinene mixture reduced the growth of *Pst*, confirming that both classes of volatile compounds led to enhanced plant resistance to *Pst* (Figure 4 A). In SA-mediated basal immunity, *EDS1* promotes SA production and *eds1* mutant plants display enhanced susceptibility to *Pst* (Feys et al., 2001). This was confirmed here by finding enhanced growth of *Pst* in mock-treated *eds1-2* compared to wt Col-0 plants (Figure 4 A). Also, *eds1* mutant plants supported reduced *Pst* growth in response to SA (Feys et al., 2001) or its volatile methylated derivative MeSA compared to the control-treated plants (Figure 4 A). By contrast, treatment of *eds1-2* mutant plants with the pinene mixture did not enhance their resistance to *Pst* growth (Figure 4 A), indicating that *EDS1* is required for the plant response to volatile pinenes. Similarly, the SA signaling mutant *npr1-1* did not respond with reduced *Pst* growth after headspace exposure to MeSA or pinenes (Figure 4 A), indicating that SA signaling is required for pinene-induced resistance. The latter trends were confirmed in additional experiments using the SA biosynthesis

mutant *sa induction deficient2-1* (*sid2-1*; Wildermuth et al., 2001). SID2 is also known as ISOCHORISMATE SYNTHASE1 (ICS1) and is part of the isochorismate biosynthetic pathway that is essential for pathogen-induced SA accumulation (Wildermuth et al., 2001; Vlot et al., 2009). In contrast to wt plants, which responded to exposure to volatile pinenes by reducing *Pst* growth, *sid2-1* mutant plants did not support pinene-induced resistance to *Pst* (Figure 4 B). Together, the data suggest that downstream processing of pinene-derived signals requires SA biosynthesis and signaling for increased plant immunity.

To assess if pinenes induce SA signaling, we analyzed the transcript accumulation of the SA marker gene *PR1* in leaves of plants exposed for 3 d to MeSA or the pinene mixture compared to that in hexane-treated plants. With both types of volatile infochemicals, we observed an increase in *PR1* expression compared to the hexane control (Figure 4 C), suggesting that the pinene mixture induces SA signaling. This observation was supported by microarray analysis in which the genome-wide transcriptional response of leaves after 3 d of exposure to volatile pinenes relative to the hexane-treated control plants was monitored (Table 1, Supplemental Dataset 1). Pinene-mediated induction of *PR1* gene expression displayed highest amplitude compared to other regulated genes. In total, the microarray analysis revealed 1214 genes with differential expression in pinene- and control-treated tissues (limma *t*-test, $P<0.05$, no fold-change cut-off; Supplemental Dataset 1). Of these, 132 genes were at least two-fold upregulated and 133 genes were at least two-fold downregulated in response to the headspace exposure with the pinene mixture compared to control-treated plants. GO enrichment analysis of the upregulated genes revealed over-representation of defense-related processes with cell death, SAR and SA signaling as well as transport representing the major components (Figure 5 A, Supplemental Dataset 2). The six most significantly regulated genes (false discovery rate-adjusted *P*-value (*Q*) < 0.05; Table 1 and Supplemental Dataset 1) were consistently upregulated in all individual biological replicates (Figure 5 B). They included the PTI-associated *FLG22-INDUCED RECEPTOR-LIKE KINASE 1* (*FRK1*; Po-Wen et al., 2013) and the *AZI1* paralogs *AZI3* and *AT4G12500* (*AZI4* in Cecchini et al., 2015). Also, we found a consistent induction of the additional *AZI1* paralog *EARLI1*, which is essential for SAR (Cecchini et al., 2015). Similarly, expression of transcription factors supporting both SA biosynthesis (*CALMODULIN-BINDING PROTEIN 60g* (*CBP60g*);

Wang et al., 2009) and SA signaling (*WRKY38*; Kim et al., 2008) was increased in the pinene treatment as well as that of *APOPLASTIC, EDS1-DEPENDENT15* (*AED15*), a chitinase (*CHI*) that we previously associated with SAR in Col-0 *DEX:AvrRpm1-HA* plants (Table 1, Figure 5 B, Breitenbach et al., 2014). Taken together, the data suggest that headspace exposure of *A. thaliana* plants to pinene induces defense-related gene expression that has significant overlap with SA and SAR-like responses.

With its paralogs *EARLI1*, *AZI3*, and *AZI4*, expression of *AZI1* was moderately and consistently induced by ~1.6-fold in the pinene- compared to control-treated plants analyzed on the microarrays (Table 1, Supplemental Dataset 1). *AZI1* is in part functionally redundant with *EARLI1* in SAR (Cecchini et al., 2015), and we sought to confirm pinene-induced transcript accumulation changes of *AZI1*, *EARLI1*, *AZI3*, and *AZI4* by RT-qPCR. Across seven biologically independent replicates, exposure of *A. thaliana* to pinenes induced *AZI1* and *EARLI1* transcript accumulation by ~4-fold compared to that in mock-treated plants and *AZI4* and *AZI3* transcript accumulation by ~6- to 8-fold, respectively (Supplemental Figure 5). *AZI1* is thought to act in a positive feedback loop with G3P, the levels of which are reduced in *gly1* (G3P dehydrogenase) mutant plants (Chanda et al., 2011; Yu et al., 2013). To investigate if *AZI1* and/or G3P are involved in monoterpene-induced resistance, we exposed *azi1-2* and *gly1-3* mutant plants to the pinene mixture for 3 d, after which plants were infected with *Pst.* In contrast to wt control plants that responded to the pinene treatment by reducing *Pst* growth compared to that in hexane/control-treated plants, *azi1-2* mutants did not respond to the pinene treatment, indicating that *AZI1* is necessary for monoterpene-induced bacterial resistance (Figure 6). By contrast, *gly1-3* mutant plants responded to the pinene mixture with *Pst* growth reduction that was comparable to that of wt plants (Figure 6). This indicates that G3P is dispensable for monoterpene-induced resistance. Together, the data suggest that *AZI1* supports immunity downstream of monoterpenes and independently of G3P.

Monoterpenes induce ROS accumulation

Exposure of *A. thaliana* to the volatile fungal sesquiterpene α-thujopsene stimulates production of superoxide anion radicals ($O_2^{\bullet-}$) in roots (Ditengou et al., 2015). Additionally, SAR depends on ROS, and the accumulation of AzA might be enhanced

by $O_2^{\bullet-}$ (Wang et al., 2014). Therefore, we assessed whether monoterpenes induce $O_2^{\bullet-}$ in *A. thaliana*. To this end, plants were exposed to the pinene mixture for 3 d, after which $O_2^{\bullet-}$ was visualized in the leaves after staining with nitroblue tetrazolium (NBT) (e.g., Ditengou et al., 2015). Similar to α-thujopsene, the pinene mixture enhanced the accumulation of $O_2^{\bullet-}$ (Figure 7), suggesting that ROS accumulate in response to treatment with the pinene mixture, as part of a relay mechanism through which these monoterpenes enhance defense.

Monoterpene biosynthesis is essential for SAR

To further test our hypothesis that volatile monoterpenes play a role in SAR, we assessed the importance of monoterpene biosynthesis in plant defense and SAR. *A. thaliana GERANYLGERANYL REDUCTASE* (*GGR*) encodes a type II small subunit of the heterodimeric GERANYL DIPHOSPHATE SYNTHASE (GPS) (Wang and Dixon, 2009; Tholl and Lee, 2011). GPS is responsible for the biosynthesis of terpene precursors including geranyl diphosphate (GPP), the main precursor of all monoterpenes (Tholl and Lee, 2011). GGR is believed to function as an “accelerator” of GPS activities and as a ‘‘modifier’’ of chain length of the product of GPS from GGPP (C_{20}) to GPP (C_{10}), specifically supporting production of (C_{10}) monoterpenes (Wang and Dixon 2009; Tholl and Lee, 2011; Yin et al, 2017). Before assessing the role of GGR in monoterpene-mediated SAR, we analyzed *GGR* transcript accumulation in two transfer DNA (T-DNA) insertion mutants, *ggr1-1* and *ggr1-2*, and in wt plants by RT-qPCR. Leaves of *ggr1-1* mutants contained very low (1.1% relative to wt) levels of *GGR* transcripts and in *ggr1-2* plants *GGR* expression was reduced by ~60% compared to the wt control (Figure 8 A). We also compared growth of a SAR-inducing *Pst AvrRpm1* inoculum in wt, *ggr1-1* and *ggr1-2* plants. Because *Pst AvrRpm1* grew to similar titers in the *ggr* mutants and wt plants at 2 and 4 dpi (Supplemental Figure 6), we concluded that these mutations do not affect local AvrRpm1-induced ETI leading to SAR.

To investigate SAR, we inoculated two lower leaves of wt, *ggr1-1*, and *ggr1-2* plants with *Pst AvrRpm1* and monitored SAR development using a challenge infection of the systemic leaves with *Pst*. At 4 dpi, *Pst* titers in systemic leaves of *Pst AvrRpm1* pre-inoculated wt plants was ~10-fold lower than in mock pre-treated plants, indicating that SAR was induced by primary *Pst AvrRpm1* infection (Figure 8 B). We did not

observe a repression of *Pst* growth in systemic leaves of the *ggr1-1* and *ggr1-2* mutants, indicating that SAR induction was abolished in the *ggr* mutant background (Figure 8 B). Similar to the local response of the mutants to *Pst AvrRpm1* (Supplemental Figure 6), the local response to *Pst* in both *ggr* mutants was similar to that of wt plants (compare *Pst* titers after the challenge infections of the mock-treated plants in Figure 8 B). These data suggest that *GGR* is essential for the induction of SAR but not for local resistance responses.

Additionally, we tested whether reduced monoterpene levels due to compromised monoterpene precursor biosynthesis are causal for defective SAR in the *ggr* mutants. Using a similar experimental regime as above, we exposed wt, *ggr1-1* and *ggr1-2* plants to MeSA or the pinene mixture. *Pst* growth was reduced in wt plants that had undergone 3 d of headspace incubation with either MeSA or pinenes compared to plants that had been treated with hexane prior to the *Pst* inoculation (Figure 8 C). Both *ggr* mutants responded to volatile MeSA by reducing *Pst* growth compared to the hexane-treated plants, arguing that *GGR* might act upstream of SA in defense signaling (Figure 8 C). More importantly, both *ggr* mutants responded normally to the pinene exposure by reducing *Pst* growth compared to the mock control (Figure 8 C). These results suggest that an external application of pinenes compensates for reduced endogenous monoterpene biosynthesis in plant defense. To further assess if a failure in monoterpene production might underlie the SAR defect in *ggr* mutant plants, we aimed to chemically complement the SAR-deficient phenotype of *ggr1-1* plants with a pinene headspace exposure. To this end, wt and *ggr1-1* mutant plants were inoculated in the first two true leaves with *Pst AvrRpm1* to induce SAR signaling. After 3 d, a secondary *Pst* inoculum was applied to the systemic tissue. Because *Pst* growth was reduced in pre-infected wt, but not *ggr1-1* mutant plants, compared to that in mock-pre-treated control plants, SAR signaling was functional in wt but not *ggr1-1* mutant plants (Figure 8 D, lanes 1, 2, 7, and 8). Chemical complementation was performed by exposing plants to 0.6 µmole of the pinene mixture for 1 d on either the first (T1), second (T2), or third (T3) day of the 3-d incubation that was used to establish SAR. As controls for the pinene treatment, naïve wt plants were incubated with the pinene mixture for 3 d (positive control) or for 1 d corresponding to either T1, T2, or T3. While *in planta Pst* growth was reduced after 3 d of headspace exposure of wt plants to the pinene mixture, *Pst* growth was

unaffected in plants that had undergone either of the 1-d treatments (Figure 8 D, lanes 3–6). However, incubation of *Pst AvrRpm1*-infected *ggr1-1* plants with the pinene mixture for 1 d restored the ability of the mutant plants to support SAR as evidenced by reduced *Pst* growth in the systemic tissue of *Pst AvrRpm1*-infected *ggr1-1* plants that were treated with the pinene mixture at T1, T2, or T3 (Figure 8 D, lanes 10–12) compared to the corresponding hexane/mock control (Figure 8 D, lane 9). Thus, pinene application complemented the SAR-defective phenotype of the *ggr1-1* mutant and this was independent of the time point of the application (Figure 8 D, lanes 10–12). Although the relationship between pinenes and SAR thus does not appear to be restricted to particular temporal events in the establishment of SAR, the data suggest that monoterpene production, emission, and/or recognition is essential for SAR.

Monoterpenes contribute to defense-related plant-to-plant communication

Because monoterpenes are highly volatile and not normally stored in *A. thaliana* cells (Tholl and Lee, 2011), we reasoned that these compounds also support defense-related plant-to-plant communication. To test this hypothesis, we incubated eight Col-0 wt *A. thaliana* receiver plants in a vacuum desiccator together with 12 mock-treated or *Pst AvrRpm1*-infected sender plants. The incubations were performed as in the headspace exposure experiment described above. After 3 d, the receiver plants were inoculated with *Pst* and *in planta Pst* titers were determined at 4 dpi. Wt receiver plants responded to co-incubation with *Pst AvrRpm1*-infected wt plants by reducing *Pst* growth compared to wt plants that had been co-incubated with mock-treated wt plants (Figure 9). This indicated that wt-to-wt communication occurs in response to *Pst AvrRpm1*, resulting in increased resistance to *Pst* in the receiver plants. However, *Pst* growth was not reduced in wt receiver plants after their co-incubation with *Pst AvrRpm1*-infected *eds1-2*, *ggr1-1*, or *ggr1-2* mutant plants compared to the corresponding mock controls (Figure 9 and Supplemental Figure 7). Thus, emissions from both *eds1-2* and *ggr* plants lack VOCs that are essential for plant-to-plant propagation of defense signaling. We hypothesized that these VOCs are monoterpenes, including camphene and α- and β-pinene, which were absent from the emissions of *avrRpm1-HA*-expressing *eds1-2* mutant plants (Figure 2 B–D). To verify this hypothesis, we measured camphene and α- and β-pinene in the emissions

of *Pst AvrRpm1*-infected wt and *ggr1-1* mutant plants, and compared them to the same emissions of mock-treated wt plants. *Pst AvrRpm1* progressively enhanced camphene and α- and β-pinene emissions from wt plants at 1 to 3 d after infection (Figure 10). By contrast, the emissions of camphene and α- and β-pinene remained at the basal (T0) level at 1 to 3 d after the mock treatment. The α-pinene and camphene emissions were significantly different between *Pst AvrRpm1*-infected and mock-treated wt plants at 3 dpi (Figure 10 A and C). PCA analysis showed that all three monoterpenes positively correlated with the observed higher emission rates (Figure 10 A–C) of *Pst AvrRpm1*-infected compared mock-treated wt plants, in particular at 3 dpi (Figure 10 D). Thus, *Pst AvrRpm1* enhanced emissions of the monoterpenes camphene and α- and β-pinene in *A. thaliana*. Importantly, camphene and α- and β-pinene could not be detected in the basal and *Pst AvrRpm1*-induced emissions of *ggr1-1* mutant plants (Figure 10). Because both *eds1-2* and *ggr1-1* plants thus showed reduced camphene and α- and β-pinene emissions (Figures 2 and 10), the ability of sender plants to emit these monoterpenes was strongly associated with plant-to-plant defense propagation (Figure 9 and Supplemental Figure 7). In contrast to monoterpenes, MeSA emissions in all samples remained below our detection limit (Supplemental Figure 8) which approximated a MeSA emission rate of ~3.2 pmol m^{-2} s^{-1}. Taken together, our data suggest that monoterpenes, in particular camphene and α- and β-pinene, have a prominent role in SAR and SAR-like signaling between plants.

Discussion

Here, we show that monoterpene emissions are essential for *A. thaliana* SAR but not for local SA-mediated immunity. Additionally, monoterpenes appear to act in plant-to-plant signaling in a manner reminiscent of SAR. *AvrRpm1-HA*-expressing *A. thaliana* plants emitted four monoterpenes and a fatty acid derivative in an *EDS1*-dependent manner, thus linking these emissions to SAR competence (Figure 1 and 2). Headspace exposure of wt *A. thaliana* to a mixture of α-pinene and β-pinene induced SA-mediated immunity against *Pst* (Figures 3–5). Reciprocally, suppression of monoterpene biosynthesis and emission in *ggr* mutant plants abolished SAR and the ability of *Pst AvrRpm1*-infected plants to trigger SAR-like immunity in neighboring wt plants (Figures 8–10). Our transcript profiling, biochemical, and genetic analysis

using *azi1* and *gly1* mutants further connected pinene-induced immunity with the SAR-associated putative lipid transfer proteins AZI1, EARLI1, and their paralogs AZI3 and AZI4, and with the accumulation of $O_2^{\bullet-}$ (Figures 5-7). This work defines monoterpenes, in particular pinenes and camphene, as volatile signaling intermediates in SAR and plant-to-plant SAR-like signal relay in *A. thaliana*.

Monoterpenes and *EDS1*-SA signaling

Early studies of the role of *EDS1* in SA-mediated resistance showed that *EDS1* promotes pathogen-induced SA accumulation and signaling (Feys et al., 2001). SA or its functional analog benzothiadiazole (BTH) induce *PR1* transcript accumulation in *eds1* mutant plants, consistent with *EDS1* acting upstream of SA (reviewed in Vlot et al., 2009). SA, in turn, enhances *EDS1* transcript accumulation, together fortifying immunity in a positive feedback loop (Figure 11). Besides boosting SA resistance, EDS1 can partially compensate for disabled SA signaling, thus further strengthening basal immunity and ETI (Cui et al., 2017). Our analysis here shows that monoterpene emissions also depend on *EDS1.* However, in contrast to SA, the pinene mixture did not significantly enhance *EDS1* expression (Supplemental Dataset 1). Nevertheless, the mixture of α- and β-pinene enhanced immunity in an *EDS1*- and SA-dependent manner (Figure 4). Previously, we showed that *EDS1* is necessary for the systemic perception of SAR signals, likely propagating immune signaling via the *EDS1*-SA positive feedback loop (Breitenbach et al., 2014). Similarly, *EDS1* action in the plant's response to pinenes might be associated with an EDS1 role in fortifying SA signaling (Figure 11). Notably, the pinene mixture enhanced expression of the *EDS1*-dependent *CBP60g* gene encoding a transcription factor that regulates expression of *ICS1* and accumulation of SA (Wang et al., 2009; Cui et al., 2017; Table 1). Together, our data suggest that pinenes promote SA signaling via an *EDS1*-SA positive feedback loop involving *CBP60g*.

EDS1-monoterpene-AzA signaling in SAR

We documented a SAR-specific role in plant immunity for the monoterpene biosynthesis-associated gene *GGR* (Figure 8). Monoterpene biosynthesis depends on the chloroplastic methylerythritol phosphate (MEP) pathway (Tholl and Lee, 2011). Also in the chloroplast, the putative phloem-mobile SAR signal AzA accumulates via

peroxidation of C_{18} membrane lipids (Zoeller et al., 2012). We show that plant exposure to pinenes triggers the accumulation of $O_2^{\bullet-}$ in wt *A. thaliana* leaves (Figure 7), while $O_2^{\bullet-}$ is one of several ROS species that stimulate the peroxidation of C_{18} unsaturated fatty acids (Zoeller et al., 2012; Wang et al., 2014). AzA is believed to promote SAR in a pathway that acts locally (in SAR signal biosynthesis or transmission) and in parallel with SA (Jung et al., 2009; Wang et al., 2014; Cecchini et al., 2015). Strikingly, SA-independent EDS1 actions upstream of AzA are also important for SAR (Breitenbach et al., 2014; Wittek et al., 2014).

A. thaliana exposure to the pinene mixture induced expression of the SAR-associated genes *AZI1* and *EARLI1* as well as their paralogs *AZI3* and *AZI4* (Table 1, Figure 5). EARLI1 and AZI3 share with AZI1 a subcellular localization to the endoplasmic reticulum (ER), plasma membrane, and the outer chloroplast membrane, in particular accumulating at ER/chloroplast contact sites (Cecchini et al., 2015). Because AZI4 shares AZI3's structural features determining its subcellular localization to ER/chloroplast contact sites (Cecchini et al., 2015), AZI4 might co-localize with AZI1, EARLI1, and AZI3. As putative lipid-transfer proteins, AZI1 and EARLI1 have been hypothesized to facilitate the intra-cellular transport of SAR-associated signals from their chloroplastic site of biosynthesis via the ER to plasma-membrane-associated apoplast or phloem loading sites for long-distance movement (Cecchini et al., 2015). In that putative function, AZI1 and EARLI1 are each required for local SAR signal emission and appear to stimulate the systemic movement of AzA (Cecchini et al., 2015). Thus, the induction of *AZI1* and its paralogs downstream of pinenes might promote immunity mediated by AzA.

Together, the regulation of AzA downstream of monoterpene biosynthesis or emission and subsequent induction of $O_2^{\bullet-}$ might be central to an *EDS1*-regulated, monoterpene-dependent, local SA-independent and SAR-specific signaling pathway (Figure 11). In parallel, this pathway relies on intact SA biosynthesis and signaling (Figure 4; Jung et al., 2009), which likely is important in the systemic tissue for an effective monoterpene- and AzA-induced immune response. Although exposure of *Pst AvrRpm1*-infected *ggr1-1* plants to the pinene mixture complemented the normally SAR-deficient phenotype of these plants (Figure 8), we cannot exclude that monoterpenes affect SAR through the air in parallel with known intra-plant SAR signaling cascades. Nevertheless, it is known that ROS promote SAR upstream of

AzA and AZI1 in a signaling cascade that acts in parallel with SA (Yu et al., 2013; Wang et al., 2014; Gao et al., 2015), and it is tempting to speculate that monoterpenes act farther upstream in this SAR-intrinsic pathway (Figure 11).

The MEP pathway in SAR

The C_{10} monoterpene precursor GPP is produced in the chloroplast as a result of the MEP pathway (Tholl and Lee, 2011). Blocking the MEP pathway by fosmidomycin, a chemical inhibitor of the second enzyme of the pathway, 2C-METHYL-D-ERYTHRITOL 4-PHOSPHATE SYNTHASE, compromised SA-mediated immunity (Gil et al., 2005). By contrast, reducing the enzyme that catalyzes the penultimate reaction in the same pathway (1-HYDROXY-2-METHYL-2-BUTENYL 4-DIPHOSPHATE SYNTHASE) enhanced SA-mediated immunity as well as jasmonic acid-associated defense responses (Gil et al., 2005; Lemos et al., 2016). This was attributed to an elevated accumulation of the upstream non-volatile intermediate MEcPP (2C-methyl-D-erythritol 2,4-cyclodiphosphate) rather than to possible volatile monoterpene products of the pathway (Gil et al., 2005). Translocated from the chloroplast to the nucleus, MEcPP acts as retrograde signal modulating the expression of stress-related genes (Xiao et al., 2012). Notably, a possible differential accumulation of the retrograde signal MEcPP cannot explain the plant-to-plant signaling phenotype documented here. Together, the data suggest a dual role of MEP pathway intermediates and products regulating innate immunity via MecPP and specifically promoting SAR through monoterpenes.

Monoterpene perception in SAR and plant-to-plant SAR-like signaling

The volatile emissions from infected *A. thaliana* plants enhanced resistance in surrounding plants to a subsequent *Pst* infection (Figure 9 and Supplemental Figure 7). This plant-to-plant SAR-like effect has been observed before in *A. thaliana* and *Nicotiana tabacum* (tobacco) but was associated with MeSA emissions only (Shulaev et al., 1997; Koo et al., 2007). Here, we observed a tight association between plant-to-plant SAR-like signaling and monoterpene emissions. Reduced α-pinene, β-pinene and camphene contents in emissions from *eds1-2* and *ggr1-1* mutant plants compromised induction of SAR-like immunity in neighboring plants, suggesting that monoterpenes are essential for this response. Other VOCs that trigger SA-mediated

immunity include MeSA and the C_9 aldehyde nonanal (Shulaev et al., 1997; Park et al., 2007; Koo et al., 2007; Yi et al., 2009). In our experiments, MeSA emissions remained below the detection limit (Supplemental Figure 8). Nonanal, the other known infochemical, was detected here and emitted at similar rates from *AvrRpm1-HA*-expressing wt and *eds1-2* mutant plants (Supplemental Table 1). *Pst AvrRpm1* progressively enhanced α-pinene, β-pinene and camphene emissions from *A. thaliana* over the course of 3 d (Figure 10), which equals the time necessary for the pinene mixture to enhance *A. thaliana* resistance to *Pst* (Figure 3). The pinene and camphene amounts needed to trigger resistance responses in the headspace exposure experiments were in the ppmv range, exceeding by ~1000-fold the concentrations recorded herein (Figures 2 and 10) and in naturally occurring forest canopies (Fuentes et al., 2007; Noe et al., 2012). However, relatively low ambient monoterpene levels do not exclude that higher concentrations can occur in the immediate vicinity of plant leaves at the forest floor or in dense canopies. Moreover, the relatively low *A. thaliana* monoterpene emissions (Figures 2 and 10) sufficed to support plant-to-plant SAR signaling (Figure 9), suggesting that monoterpenes, in particular pinenes and camphene, provide essential reinforcement to other signals, which might include nonanal and MeSA, in the volatile infochemical emission pattern of *Pst AvrRpm1*-infected plants.

The chemical properties of (mono)terpenes allow these molecules to diffuse through the apolar, waxy cuticle of plant leaves (Schmid et al., 1992). Depending on the atmospheric concentration, monoterpenes can accumulate in other plants (e.g., Spielmann et al. 2016). For example, terpenes emitted by *Rhododendron tomentosum* were found in the leaf cuticles of neighboring birch (*Betula spp.*) trees (Himanen et al., 2010). It is thus possible that volatile monoterpenes emitted from local infected leaves are absorbed by the cuticles of systemic leaves of the same or neighboring plants. It is interesting to note that SAR is abolished in *acyl carrier protein4* (*acp4*) mutant plants, which also exhibit reduced cuticular wax and cutin formation (Xia et al., 2009). *ACP4* supports systemic SAR signal perception and thus might be important for the absorption of volatile signals, including monoterpenes. After their uptake via the cuticle (or stomata), monoterpenes (likely as components of natural plant-emitted VOC blends) trigger defense signaling at least in part via the induction of $O_2^{\bullet-}$ (Figures 7 and 11). Additionally, AZI1 and its paralogs might

contribute to the early perception of monoterpenes (Figures 6 and 11). In addition to the well-established role of AZI1 in the regulation of local SAR signal emission (Jung et al., 2009; Wang et al., 2014; Cecchini et al., 2015), Lim et al. (2016) recently reported evidence for an additional function of AZI1 in systemic SAR signal perception. It is possible that monoterpenes act upstream of this systemic function of AZI1 in SAR signal perception within and between plants.

Plant VOCs have long been recognized as plant-to-plant signaling molecules, allowing plants undergoing a particular stress to warn their neighbors. Until now, plant-to-plant signaling was mostly studied with respect to plant-insect interactions and abiotic stress responses (Scala et al., 2013a; Pierik et al., 2014; Dong et al., 2016). However, an increasing number of plant-derived and other (microbial/fungal) biogenic VOCs has been associated with SA signaling over the past ten years (Yi et al., 2009; Junker and Tholl, 2013; Choi et al., 2014; Naznin et al., 2014; Song et al., 2015), suggesting an ecological importance of VOC-mediated communication between organisms in plant innate immunity. The diterpene DA likely acts as a systemic mobile non-volatile signal in *A. thaliana* SAR (Chaturvedi et al., 2012), while another diterpene compound has been associated with SA-mediated resistance responses in tobacco (Seo et al., 2003). A connection between monoterpene accumulation and SA-mediated defenses was documented in bean and orange (Arimura et al., 2000; Rodríguez et al., 2014). In lima beans (*Phaseolus lunatus*), exogenously applied ocimene induced SA-associated defense genes (Arimura et al. 2000). In orange (*Citrus* × *sinensis*), monoterpene downregulation enhanced jasmonic acid-associated defense responses, while SA was induced in response to *Penicillium digitatum* in orange fruits normally accumulating the monoterpene limonene (Rodríguez et al., 2014). Similar to MeSA, the emissions of α-pinene and sabinene from *A. thaliana* are induced by methyl jasmonate (Kegge et al., 2013). However, a physiological role of bicyclic monoterpenes, such as α- or β-pinene, in plant responses to stress has not been reported so far. The current work provides the first evidence linking bicyclic monoterpenes to plant immunity. More specifically, these volatile signaling molecules are important for SAR and might function as infochemicals mediating SAR-like responses between plants. In an ecological context, monoterpenes might allow plants to recognize signals from plants of the

same or other species (Dicke, 2009; Dicke and Baldwin, 2010; Pierik et al., 2014; Pickett and Khan, 2016) leading to SAR. Preliminary data suggest that the monoterpene emissions from Norway spruce (*Picea abies*) needles (Ghirardo et al., 2010) enhance defense in *A. thaliana* against *P. syringae* (Supplemental Figure 9). Hence, plant-to-plant SAR-like signaling, in which monoterpenes play a role, will be subject to future studies in homogeneous and mixed plant settings.

Methods

Plant materials and growth conditions

All experiments were performed in the *A. thaliana* ecotype Columbia-0 (Col-0). Mutants *eds1-2*, *npr1-1*, *sid2-1*, and *azi1-2* as well as Col-0 *pDEX:AvrRpm1-HA* and *eds1-2 pDEX:AvrRpm1-HA* plants were previously described (Cao et al., 1997; Wildermuth et al., 2001; Mackey et al., 2002; Bartsch et al., 2006; Jung et al., 2009; Breitenbach et al., 2014). The T-DNA insertion lines SALK_208952C (*ggr1-1*) and SALK_210207C (*ggr1-2*) were obtained from the Nottingham Arabidopsis Stock Centre (Scholl et al., 2000). Seeds of selected homozygous plants were used for the experiments. Plants were grown as described previously (Breitenbach et al., 2014). Two weeks after germination, plants were watered once with Biomükk (Bio-Farming-Systems AG, Münsingen, Germany) according to the manufacturer's instructions. Four- to five-week-old plants were used for all experiments. For VOC application and plant-to-plant communication experiments, plants were grown in stainless steel pots (Rotilabo-Messbecher high-grad steel, ∅ 30mm, Roth, Karlsruhe, Germany).

Pathogens and infections

Pst and *Pst* carrying the bacterial effector AvrRpm1 (*Pst AvrRpm1*) were maintained as described (Breitenbach et al., 2014). SAR was induced with a primary infection of the first two true leaves with *Pst AvrRpm1* as described (Breitenbach et al., 2014). For challenge infections, two upper leaves of control-treated, SAR-induced, or VOC-treated plants were syringe-infiltrated with 10^5 colony forming units (cfu) per mL of *Pst*. *Pst* growth was monitored at 4 dpi as described earlier (Breitenbach et al., 2014). Similarly, the *in planta Pst AvrRpm1* growth was monitored after inoculation of fully expanded leaves with 10^5 cfu per mL of the bacteria. Finally, spray inoculations

were performed with 10^8 cfu/mL of *Pst AvrRpm1* in 0.01% Tween-20 (v:v) and compared to mock treatments with 0.01% Tween-20 (v:v).

Chemical treatments

All chemicals were purchased from Sigma (Deisenhofen, Germany) and Roth. For VOC measurements, Col-0 and *eds1-2* plants carrying *pDEX:AvrRpm1-HA* were sprayed until drop-off with 30 µM DEX in 0.01% (v:v) Tween-20. VOC treatments were performed in 5.5 L gas-tight glass desiccators (Rotilabo-Glas-Exsikkatoren, Roth). The desiccators were filled with eight pots/plants, a filter paper for VOC application, and fresh air from the inflow of the growth chamber. For the treatments, 200 µL of hexane was supplemented with different amounts of VOCs (ranging from ~0.1 to ~1.4 µmole, maximally evaporating to form concentrations in the air ranging from ~350 parts per billion by volume (ppbv) to ~6 parts per million by volume (ppmv) in the desiccator). All VOC solutions were prepared freshly in 300 µL gas-tight glass (HPLC) vials and applied to a filter paper in the desiccators using an HPLC-syringe and the desiccator gas tap. As a negative control, 200 µL of hexane alone was used. The plants were incubated for 3 d, during which the supplemented air, including the applied treatment, was replaced every 24 h. After 3 d, the plants were removed from the desiccators and two fully expanded leaves were either harvested for further analysis or challenged with *Pst* as described above.

Plant-to-plant communication

Plant-to-plant communication was analyzed in 5.5 L gas-tight glass desiccators (Rotilabo-Glas-Exsikkatoren, Roth). Stainless steel pots containing three plants each were sprayed with 10^8 cfu/mL of *Pst AvrRpm1* in 0.01% Tween-20 (v:v) and allowed to dry for 1 h. A corresponding mock treatment was performed with 0.01% Tween-20 (v:v). Subsequently, four treated pots were enclosed per dessicator together with four pots containing two wt ‘receiver’ plants each. The plants were incubated for 3 d, during which the dessicators were opened every 24 h to let in fresh air. Subsequently, the ‘receiver’ plants were challenged with *Pst* as described above.

VOC collection and analysis

VOCs that were emitted from DEX-treated plants were collected in two sampling intervals from 1 to 4 h and from 4 to 7 h after DEX treatment in eight cuvettes (~4.2 L) that were run in parallel. The plants were acclimatized to the cuvettes overnight prior to the DEX treatment and VOC collection. The cuvettes were made of glass except for their base, which was made of Plexiglas. The cuvettes were 13 cm in height and had the shape of a frustum with upper and lower base diameters of 13 and 26.9 cm, respectively. Twelve plants were enclosed in each cuvette, and the cuvettes were continuously flushed with 0.2 L min^{-1} of VOC-free synthetic air (79% N_2, 21% O_2) mixed with pure CO_2 to a final concentration of 400 µmole CO_2 $mole^{-1}$ synthetic air. Inside the cuvettes, temperature, light intensity and relative humidity (night/day) were 22.3±0.3/23.7±0.7°C, 0±2/135±15 µmole photons m^{-2} s^{-1} photosynthetic active radiation (10 h-photoperiod), and 92±2/50±15% relative humidity, respectively. A part of the air exiting the cuvettes was diverted using Teflon t-pieces and the VOCs were collected at a flow rate of 0.1 L min^{-1} for 180 min (i.e., 18 L air sample) into glass cartridges filled with polydimethylsiloxane-foam (PDMS, Gerstel, Mülheim an der Ruhr, Germany) and 50 mg Carbopack B (mesh size 20/40; Sigma-Aldrich) adsorbents and 250 pmol δ-2-carene as internal standard. The inlet airflows were controlled using needle valves and measured before and after each measurement using a calibrated mass flow meter (ADM 3000, Agilent Technologies, Palo Alto, CA, USA). Background measurements were performed twice, at the beginning and at the end of the experiments. For this, DEX-treated plants were removed from the soil immediately before enclosing the pots in the cuvettes. The final analysis included 16 background replicates and 18 to 21 VOC replicates per plant genotype. Biological replicates were collected in separate cuvettes and no more than four cuvettes were used at the same time per plant genotype. In doing so, the replicates were performed across five to six separate plant batches.

VOCs from *Pst AvrRpm1*-infected and mock-treated plants were collected as described above except that VOCs were collected for 8 h per sampling time point, which included one day before and three consecutive days after the treatments of 40 plants per cuvette. The final analysis of this experiment included 8 background replicates and 7 to 10 VOC (biological) replicates from two independent plant batches per treatment and genotype.

The VOC samples were analyzed with a thermo-desorption unit (TDU, Gerstel GmbH, Mülheim, Germany) coupled to a GC-MS instrument (GC type: 7890A; MS type: 5975C Agilent Technologies, Palo Alto, CA, USA). The TDU-GC-MS measurements and analyses, including the chemical identifications corresponding to the GC-MS peaks, followed established procedures (Ghirardo et al., 2012, 2016; Weikl et al., 2016). Only the GC-MS temperature program was slightly modified: 40°C for 0 min, followed by ramping at 10°C min^{-1} to 130°C and holding for 5 min, followed by ramping at 80°C min^{-1} to 175°C and holding for 0 min, followed by ramping at 2°C min^{-1} to 200°C and holding for 0 min, followed by ramping at 4°C min^{-1} to 220°C and holding for 0 min, followed by ramping at 100°C min^{-1} to 300°C and holding for 6 min.

Analysis of GC-MS Data

VOCs were quantified and identified as described previously (Ghirardo et al, 2012, 2016). For background correction, all quantified GC-MS peaks observed in plant-derived samples were subtracted by the mean values of the corresponding peaks originating from the background measurements. After background correction, emission rates of VOCs were calculated on a projected rosette area basis (pmol m^{-2} s^{-1}). For rosette area determination, all plants had been photographed with a fixed installed camera system prior to the treatments, and the projected rosette areas were quantified using picture pixels (www.gimp.org).

The VOC data were statistically analyzed by MDA using principal component analysis (PCA) and PLSR as previously described (Ghirardo et al., 2016; Jud et al., 2016; Weikl et al., 2016) using the software package SIMCA-P version 13.0.0.0 (Umetrics, Umeå, Sweden). Before MDA, data were pre-processed by log transformation [X = log(X+min)], mean centered, and scaled to unit variance. Cross-validation was used to validate the number of significant PCA and PLSR components (Eriksson et al., 2006) using a 99% confidence level on parameters and seven cross-validation groups.

For the analysis of the data derived from DEX-treated plants, PCA was used for the initial exploration of the dataset and the detection of outliers (Ghirardo et al., 2005), ensuring an objective and unsupervised analysis. Subsequently, OPLS was

performed using as X-variables all non-background corrected (but normalized to internal standard) data, including VOCs collected from both plant and background measurements. The Y-variables described in a binary mode the sample collected from plants (Y=1) and those from background (Y=0). Of the initial 137 peaks, 39 peaks were statistically and positively correlated to plant emissions. The remaining 98 peaks were associated with background and therefore discarded in the following analyses. For further analyses, background-corrected VOC emission rates of the 39 plant-derived peaks from each sample were used as X-variables. OPLS was performed using samples from SP1 and SP2 separately, aiming to correlate VOCs to the two different genotypes, Col-0 (Y=0) and *eds1-2* (Y=1) independent of the sampling periods.

The OPLS results were validated using analysis of variance testing of cross-validated predictive residuals (CV-ANOVA; Eriksson et al., 2008). The overall analysis aimed to identify if and at which degree the emission potentials of VOCs positively or negatively correlated to the plant genotype *eds1-2*. A volatile compound was classified discriminant when both (i) importance in the projection was higher than 1 (VIP>1) and (ii) the uncertainty bar computed by jack-knife method (Efron and Gong, 1983) was smaller than its respective VIP value. Finally, the emission rates of the VOCs that were discriminant for plant genotype were additionally challenged by Student`s *t*-test.

NBT staining

Leaves of pinene- and control-treated plants were stained with NBT essentially as described (Ditengou et al., 2015) with the following modifications: NBT was kept in the leaves for 20 minutes prior to destaining. After destaining, the leaves were cleared in 100% ethanol for 15 minutes and subsequently in 80% ethanol for 30 minutes, each at 80°C. Finally, the leaves were kept in 30% glycerol and photographed with a fixed camera system. The pixels were quantified with ImageJ.

RNA isolation and RT-qPCR analysis

RNA isolation, cDNA synthesis, and SYBR Green-based quantitative PCR (qPCR) using primers for *PR1* and *UBIQUITIN* (*UBI*) were performed as described

(Breitenbach et al., 2014). The nucleotide sequences of the other qPCR primers used in this study are listed in Supplemental Table 2.

Microarray analysis For each plant treatment, RNA from four biologically independent samples, each containing material from four plants, was analyzed on 8×60K custom Arabidopsis microarrays (Design ID 29132, Agilent Technologies, USA; A-GEOD-16892) that were used for one-color gene expression analysis (Low Input Quick Amp Labeling; Agilent Technologies). All procedures were performed strictly according to the manufacturer's instructions. The data were extracted using Agilent Feature Extraction Software (version 9) with template GE1_1010_Sep10. The data were analyzed with R, version 3.0.3, using the Bioconductor package limma, version 3.18.13 (Smyth, 2004; Ritchie et al., 2015). After background correction, quantile normalization and $\log_2$ transformation, expression values of probes were averaged according to TAIR10 annotation, resulting in expression information for 24,606 genes. Differential expression analysis was performed using a linear model with the plant treatment as fixed effect and the experimental block as a random effect. For GO enrichment analysis, the function fisher.test was applied and false discovery rate-based multiple testing correction was done with p.adjust. The GO annotation and description of genes was taken from the org.At.tair.db package, version 2.10.1. In addition, GO annotation at TAIR based on literature and INTERPRO domain matches (Berardini et al., 2004) was downloaded from https://www.arabidopsis.org/download_files/GO_and_PO_Annotations/Gene_Ontology_Annotations/ATH_GO_GOSLIM.txt on Apr 26th 2016 and used to annotate the list of differentially expressed genes with terms from the domain "Biological Process". Gene aliases were taken from https://www.arabidopsis.org/download_files/Genes/gene_aliases_20130831.txt (version 2015-01-29 downloaded on Aug 31st 2016). The visualization of nonredundant significantly enriched GO terms was performed with ggplot2 (Wickham, 2009). The shown GO terms were restricted to those annotated by TAIR, and the color scheme was derived from inclusion relationships between the annotated gene lists of each term: nodes have the same color as the most specific ancestor node that includes them; the number of colors corresponds to the number of nodes not included in any other node.

Microarray data are available in the ArrayExpress database (www.ebi.ac.uk/arrayexpress) under accession number E-MTAB-5475.

Accession Numbers

The sequence of *GERANYLGERANYL REDUCTASE* (*GGR*) can be found under accession number NM_120007 (NCBI) or At4g38460 (TAIR).

Supplemental Data

Supplemental Figure 1. Pinene-induced resistance to *Pst* remains stable for one to three days after treatment.

Supplemental Figure 2. Methyl salicylate, a mixture of (±)α- and (-)β-pinene (v:v=1:1), and camphene are not toxic to *Pseudomonas syringae* pathovar *tomato.*

Supplemental Figure 3. Chemical composition of the methyl salicylate, (±)α-pinene, (-)β-pinene, (+)β-pinene, and camphene standards.

Supplemental Figure 4. Limonene headspace exposure enhances *A. thaliana* resistance to *Pst* growth.

Supplemental Figure 5. Pinene-induced *AZI1*, *EARLI1*, *AZI3*, and *AZI4* transcript accumulation in *A. thaliana* leaves.

Supplemental Figure 6. *Pst AvrRpm1* growth in wt, *ggr1-1*, and *ggr1-2* plants.

Supplemental Figure 7. Monoterpenes are important for plant-to-plant SAR signaling

Supplemental Figure 8. MeSA emissions from *Pst AvrRpm1*-infected Col-0 wt and *ggr1-1* mutant plants remained below the limit of detection.

Supplemental Figure 9. Spruce needle emissions enhance *A. thaliana* resistance to *Pst* growth.

Supplemental Table 1. VOCs in the emissions of DEX-treated Col-0 *DEX:AvrRpm1-HA* and *eds1-2 DEX:AvrRpm1-HA* plants.

Supplemental Table 2. Oligonucleotides used in this study.

Supplemental Dataset 1. Summary of microarray analysis: differentially expressed genes in pinene-treated compared to control-treated samples.

Supplemental Dataset 2. Gene Ontology (GO) terms enriched within the pinene-upregulated genes.

Acknowledgements

We thank Nadine Stefan for technical support and Dr. J. Barbro Winkler for discussion. This work was funded in part by the Deutsche Forschungsgemeinschaft (DFG) as part of SFB924 and by the German Federal Ministry of Education and Research as part of the German Plant Phenotyping Network (DPPN, no. 031A053C). JEP acknowledges The Max-Planck Society and Cluster for Excellence in Plant Sciences (CEPLAS).

Author contributions

JEP, JPS, and ACV conceived the research; MR, AG, MW, JPS, and ACV designed the research; MR, AG, MW, CK, and KK performed the research, EG customized the computational analysis of microarray data; MR, AG, MW, EG, SD, and ACV analyzed the data, ACV wrote the manuscript; MR, AG, SD, EG, JEP, and JPS contributed to the first draft; and all authors contributed to the final version of this work.

References

Aarts, N., Metz, M., Holub, E., Staskawicz, B.J., Daniels, M.J., and Parker, J.E. (1998). Different requirements for *EDS1* and *NDR1* by disease resistance genes define at least two *R* gene-mediated signaling pathways in *Arabidopsis*. Proc. Natl. Acad. Sci. U.S.A. 95: 10306-10311.

Arimura, G., Ozawa, R., Shimoda, T., Nishioka, T., Boland, W., and Takabayashi, J. (2000). Herbivory-induced volatiles elicit defence genes in lima bean leaves. Nature 406: 512–515.

Bartsch, M.E., Gobbato, E., Bednarek, P., Debey, S., Schultze, J.L., Bautor, J., and Parker, J.E. (2006). Salicylic acid-independent ENHANCED DISEASE SUSCEPTIBILITY1 signaling in Arabidopsis immunity and cell death is regulated by the monooxygenase FMO1 and the nudix hydrolase NUDT7. Plant Cell 18: 1038-1051.

Berardini, T.Z., Mundodi, S., Reiser, R., Huala, E., Garcia-Hernandez, M., Zhang, P., Mueller, L.M., Yoon, J., Doyle, A., Lander, G., Moseyko, N., Yoo, D., Xu, I., Zoeckler, B., Montoya, M., Miller, N., Weems, D., and Rhee S.Y. (2004). Functional annotation of the Arabidopsis genome using controlled vocabularies. Plant Physiol. 135: 745-755.

Breitenbach, H.H., Wenig, M., Wittek, F., Jordá, L., Maldonado-Alconada, A.M., Sarioglu, H., Colby, T., Knappe, C., Bichlmeier, M., Pabst, E., Mackey, D., Parker, J.E., and Vlot, A.C. (2014). Contrasting roles of apoplastic aspartyl protease AED1 and legume lectin-like protein LLP1 in Arabidopsis systemic acquired resistance. Plant Physiol. 165: 791-809.

Cao, H., Glazebrook, J., Clarke, J.D., Volko, S., and Dong, X. (1997). The Arabidopsis NPR1 gene that controls systemic acquired resistance encodes a novel protein containing ankyrin repeats. Cell 88: 57-63.

Cecchini, N.M., Steffes, K., Schläppi, M.R., Gifford, A.N., and Greenberg, J.T. (2015). *Arabidopsis* AZI1 family proteins mediate signal mobilization for systemic defence priming. Nat. Commun. 6: 7658.

Champigny, M.J., Isaacs, M., Carella, P., Faubert, J., Fobert, P.R., and Cameron, R.K. (2013). Long distance movement of DIR1 and investigation of the role of DIR1-like during systemic acquired resistance in *Arabidopsis.* Front. Plant Sci. 4: 230.

Chanda, B., Xia, Y., Mandal, M.K., Yu, K., Sekine, K.T., Gao, Q.M., Selote, D., Hu, Y., Stromberg, A., Navarre, D., Kachroo, A., and Kachroo, P. (2011). Glycerol-3-phosphate is a critical mobile inducer of systemic immunity in plants. Nat. Genet. 43: 421-427.

Chaturvedi, R., Venables, B., Petros, R.A., Nalam, V., Li, M., Wang, X., Takemoto, L.J., and Shah, J. (2012). An abietane diterpenoid is a potent activator of systemic acquired resistance. Plant J. 71: 161-172.

Choi, H.K., Song, G.C., Yi, H., and Ryu, C.M. (2014). Field evaluation of the bacterial volatile derivative 3-pentanol in priming for induced resistance in pepper. J. Chem. Ecol. 40: 882-892.

Cui, H., Gobbato, E., Kracher, B., Qiu, J., Bautor, J., and Parker, J.E. (2017). A core function of EDS1 with PAD4 is to protect the salicylic acid defense sector in Arabidopsis immunity. New Phytol. 213: 1802-1817.

Cui, H., Tsuda, K., and Parker, J.E. (2015). Effector-triggered immunity: from pathogen perception to robust defense. Annu. Rev. Plant Biol. 66: 487-511.

Dangl, J.L., Ritter, C., Gibbon, M.J., Mur, L.A.J., Wood, J.R., Goss, S., Mansfield, J., Taylor, J.D., and Vivian, A. (1992). Functional homologs of the Arabidopsis *RPM1* disease resistance gene in bean and pea. Plant Cell 4: 1359-1369.

Dempsey, D.A., and Klessig, D.F. (2012). SOS – too many signals for systemic acquired resistance? Trends Plant Sci. 17: 538-545.

Dicke, M. (2009). Behavioural and community ecology of plants that cry for help. Plant Cell Environ. 32: 654-665.

Dicke, M., and Baldwin, I.T. (2010). The evolutionary context for herbivore induced plant volatiles: beyond the 'cry for help'. Trends Plant Sci. 15: 167-175.

Ditengou, F.A., Müller, A., Rosenkranz, M., Felten, J., Lasok, H., Van Doorn, M.M., Legué, V., Palme, K., Schnitzler, J.P., and Polle, A. (2015). Volatile signalling by sesquiterpenes from ectomycorrhizal fungi reprogrammes root architecture. Nat. Commun. 6: 6279.

Dong, F., Fu, X., Watanabe, N., Su, X., and Yang, Z. (2016). Recent advances in the emission and functions of plant vegetative volatiles. Molecules 21: 124.

Efron, B., and Gong, G. (1983). A leisurely look at the bootstrap, the jackknife, and cross-validation. American Statistician 37: 36–48.

Eriksson, L., Johansson, E., Kettaneh-Wold, N., Trygg, J., Wikström, C., and Wold, S. (2006). Multi- and megavariate data analysis. Part I: basic principles and applications. Umea, Sweden: Umetrics Academy.

Eriksson, L., Trygg, J., and Wold, S. (2008). CV-ANOVA for significance testing of PLS and OPLS models. J. Chemom. 22: 594–600.

Feys, B.J., Moisan, L.J., Newman, M.A., and Parker, J.E. (2001). Direct interaction between the Arabidopsis disease resistance signaling proteins, EDS1 and PAD4. EMBO J. 20: 5400-5411.

Feys, B.J., Wiermer, M., Bhat, R.A., Moisan, L.J., Medina-Escobar, N., Neu, C., Cabral, A., and Parker, J.E. (2005). *Arabidopsis* SENESCENCE-ASSOCIATED GENE101 stabilizes and signals within an ENHANCED DISEASE SUSCEPTIBILITY1 complex in plant innate immunity. Plant Cell 17: 2601-2613.

Finefield, J.M., Sherman, D.H., Kreitman, M., and Williams, R.M. (2012). Enantiomeric natural products: Occurrence and biogenesis. Angew. Chem. Int. Ed. Engl. 51: 4802–4836.

Fu, Z.Q., and Dong, X. (2013). Systemic acquired resistance: turning local infection into global defense. Annu. Rev. Plant Biol. 64: 7.1-7.25.

Fuentes, J.D., Wang, D., Bowling, D.R., Potosnak, M., Monson, R.K., Goliff, W.S., Stockwell, W.R. (2007) Biogenic hydrocarbon chemistry within and above a mixed deciduous forest. J. Atmos. Chem. 56: 165-185.

Gao, Q.M., Zhu, S., Kachroo, P., and Kachroo, A. (2015). Signal regulators of systemic acquired resistance. Front Plant Sci. 13: 228.

García, A.V., Blanvillain-Baufumé, S., Huibers, R.P., Wiermer, M., Li, G., Gobbato, E., Rietz, S., and Parker, J.E. (2010). Balanced nuclear and cytoplasmic activities of EDS1 are required for a complete plant innate immune response. PLoS Pathog. 6: e1000970.

Ghirardo, A., Heller, W., Fladung, M., Schnitzler, J.P., and Schroeder, H. (2012). Function of defensive volatiles in pedunculate oak (*Quercus robur*) is tricked by the moth *Tortrix viridana*. Plant Cell Environ. 35: 2192–2207.

Ghirardo, A., Koch, K., Taipale, R., Zimmer, I., Schnitzler, J.P., and Rinne, J. (2010). Determination of de novo and pool emissions of terpenes from four common boreal/alpine trees by $^{13}CO_2$ labelling and PTR-MS analysis. Plant Cell Environ. 33: 781-792.

Ghirardo, A., Sørensen, H.A., Petersen, M., Jacobsen, S., and Søndergaard, I. (2005). Early prediction of wheat quality: analysis during grain development using mass spectrometry and multivariate data analysis. Rapid Commun. Mass Spectrom. 19: 525-532.

Ghirardo, A., Xie, J., Zheng, X., Wang, Y., Grote, R., Block, K., Wildt, J., Mentel, T., Kiendler-Scharr, A., Hallquist, M., Butterbach-Bahl, K., and Schnitzler, J.P. (2016). Urban stress-induced biogenic VOC emissions and SOA-forming potentials in Beijing. Atmos. Chem. Phys. 16: 2901–2920.

Gil, M.J., Coego, A., Mauch-Mani, B., Jorda, L., and Vera, P. (2005). The Arabidopsis *csb3* mutant reveals a regulatory link between salicylic acid-mediated disease resistance and the methyl-erythritol 4-phosphate pathway. Plant J. 44: 155–166.

Heil, M., and Ton, J. (2008). Long-distance signalling in plant defence. Trends Plant Sci. 13: 264-272.

Himanen, S.J., Blande, J.D., Klemola, T., Pulkkinen, J., Heijari, J., and Holopainen, J.K. (2010). Birch (*Betula* spp.) leaves adsorb and re-release volatiles specific to neighbouring plants--a mechanism for associational herbivore resistance? New Phytol. 186: 722-732.

Jing, B., Xu, S., Xu, M., Li, Y., Li, S., Ding, J., and Zhang, Y. (2011). Brush and spray: a high-throughput systemic acquired resistance assay suitable for large-scale genetic screening. Plant Physiol. 157: 973-980.

Jones, J.D., and Dangl, J.L. (2006). The plant immune system. Nature 444: 323-329.

Jud, W., Vanzo, E., Li, Z., Ghirardo, A., Zimmer, I., Sharkey, T.D., Hansel, A., and Schnitzler, J.P. (2016). Effects of heat and drought stress on post-illumination bursts of volatile organic compounds in isoprene-emitting and non-emitting poplar. Plant Cell Environ. 39: 1204-1215.

Jung, H.W., Tschaplinski, T.J., Wang, L., Glazebrook, J., and Greenberg, J.T. (2009). Priming in systemic plant immunity. Science 324: 89-91.

Junker, R.R., and Tholl, D. (2013). Volatile organic compound mediated interactions at the plant-microbe interface. J. Chem. Ecol. 39: 810-825.

Kegge, W., Weldegergis, B.T., Soler, R., Vergeer-Van Eijk, M., Dicke, M., Voesenek, L.A.C.J., and Pierik, R. (2013). Canopy light cues affect emission of constitutive and methyl jasmonate-induced volatile organic compounds in *Arabidopsis thaliana.* New Phytol. 200: 861-874.

Kim, K.C., Lai, Z., Fan, B., and Chen, Z. (2008). Arabidopsis WRKY38 and WRKY62 transcription factors interact with histone deacetylase 19 in basal defense. Plant Cell 20: 2357-2371.

Koo, Y.J., Kim, M.A., Kim, E.H., Song, J.T., Jung, C., Moon, J.K., Kim, J.H., Seo, H.S., Song, S.I., Kim, J.K., Lee, J.S., Cheong, J.J., and Choi, Y.D. (2007). Overexpression of salicylic acid carboxyl methyltransferase reduces salicylic acid-mediated pathogen resistance in *Arabidopsis thaliana.* Plant Mol. Biol. 64: 1-15.

Lemos, M., Xiao, Y., Bjornson, M., Wang, J.Z., Hicks, D., De Souza, A., Wang, C.Q., Yang, P., Ma, S., Dinesh-Kumar, S., and Dehesh, K. (2016). The plastidial retrograde signal methyl erythritol cyclopyrophosphate is a regulator of salicylic acid and jasmonic acid crosstalk. J. Exp. Bot. 67: 1557-1566.

Lim, G.H., Shine, M.B., De Lorenzo, L., Yu, K., Cui, W., Navarre, D., Hunt, A.G., Lee, J.Y., Kachroo, A., and Kachroo, P. (2016). Plasmodesmata localizing proteins regulate transport and signaling during systemic acquired immunity in plants. Cell Host Microbe 19: 541-549.

Macho, A.P., and Zipfel, C. (2014). Plant PRRs and the activation of innate immune signaling. Mol. Cell 54: 263–272.

Mackey, D., Holt, B.F., Wiig, A., and Dangl, J.L. (2002). RIN4 interacts with *Pseudomonas syringae* type III effector molecules and is required for RPM1-mediated resistance in Arabidopsis. Cell 108: 743–754.

Maldonado, A.M., Doerner, P., Dixon, R.A., Lamb, C.J., and Cameron, R.K. (2002). A putative lipid transfer protein involved in systemic resistance signalling in Arabidopsis. Nature 419: 399-403.

Mur, L.A., Kenton, P., Lloyd, A.J., Ougham, H., and Prats, E. (2008). The hypersensitive response; the centenary is upon us but how much do we know? J. Exp. Bot. 59: 501-520.

Návarová, H., Bernsdorff, F., Döring, A.C., and Zeier, J. (2012). Pipecolic acid, an endogenous mediator of defense amplification and priming, is a critical regulator of inducible plant immunity. Plant Cell 24: 5123-5141.

Naznin, H.A., Kiyohara, D., Kimura, M., Miyazawa, M., Shimizu, M., and Hyakumachi, M. (2014). Systemic resistance induced by volatile organic compounds emitted by plant growth-promoting fungi in *Arabidopsis thaliana*. PLoS One 9: e86882.

Noe, S.M., Hüve, K., Niinemets, Ü., and Copolovici, L. (2012). Seasonal variation in vertical volatile compounds air concentrations within a remote hemiboreal mixed forest. Atmos. Chem. Phys. 12: 3909-3926.

Park, S.W., Kaimoyo, E., Kumar, D., Mosher, S., and Klessig, D.F. (2007). Methyl salicylate is a critical mobile signal for plant systemic acquired resistance. Science 318: 113-116.

Pickett, J.A., and Khan, Z.R. (2016). Plant volatile-mediated signalling and its application in agriculture: successes and challenges. New Phytol. 212: 856-870.

Pierik, R., Ballaré, C.L., and Dicke, M. (2014). Ecology of plant volatiles: taking a plant community perspective. Plant Cell Environ. 37: 1845-1853.

Po-Wen, C., Singh, P., and Zimmerli, L. (2013). Priming of the Arabidopsis pattern-triggered immunity response upon infection by necrotrophic *Pectobacterium carotovorum* bacteria. Mol. Plant Pathol. 14: 58–70.

Rietz, S., Stamm, A., Malonek, S., Wagner, S., Becker, D., Medina-Escobar, N., Vlot, A.C., Feys, B.J., Niefind, K., and Parker, J.E. (2011). Different roles of enhanced disease susceptibility1 (EDS1) bound to and dissociated from phytoalexin deficient4 (PAD4) in Arabidopsis immunity. New Phytol. 191: 107-119.

Ritchie, M.E., Phipson, B., Wu, D., Hu, Y., Law, C.W., Shi, W., and Smyth, G.K. (2015). Limma powers differential expression analyses for RNA-sequencing and microarray studies. Nucleic Acids Res. 43: e47.

Rodríguez, A., Shimada, T., Cervera, M., Alquézar, B., Gadea, J., Gómez-Cadenas, A., De Ollas, C.J., Rodrigo, M.J., Zacarías, L., and Peňa, L. (2014). Terpene down-regulation triggers defense responses in transgenic orange leading to resistance against fungal pathogens. Plant Physiol. 164: 321-339.

Scala, A., Allmann, S., Mirabella, R., Haring, M.A., and Schuurink, R.C. (2013a). Green leaf volatiles: a plant's multifunctional weapon against herbivores and pathogens. Int. J. Mol. Sci. 14: 17781-17811.

Scala, A., Mirabella, R., Mugo, C., Matsui, K., Haring, M.A., and Schuurink, R.C. (2013b). *E*-2-hexenal promotes susceptibility to *Pseudomonas syringae* by activating jasmonic acid pathways in Arabidopsis. Front. Plant Sci. 4: 74.

Schmid, C., Steinbrecher, R., and Ziegler, H. (1992). Partition coefficients of plant cuticles for monoterpenes. Trees 6: 32-36.

Scholl, R.L., May, S.T., and Ware, D.H. (2000). Seed and molecular resources for Arabidopsis. Plant Physiol. 124: 1477-80.

Seo, S., Seto, H., Koshino, H., Yoshida, S., and Ohashi, Y. (2003). A diterpene as an endogenous signal for the activation of defense responses to infection with tobacco mosaic virus and wounding in tobacco. Plant Cell 15: 863-873.

Shah, J., Chaturvedi, R., Chowdhury, Z., Venables, B., and Petros, R.A. (2014). Signaling by small metabolites in systemic acquired resistance. Plant J. 79: 645-658.

Shulaev, V., Silverman, P., and Raskin, I. (1997). Airborne signalling by methyl salicylate in plant pathogen resistance. Nature 385: 718-721.

Smyth, G.K. (2004). Linear models and empirical Bayes methods for assessing differential expression in microarray experiments. Stat. Appl. Genet. Mol. Biol. 3: 3.

Song, G.C., Choi, H.K., and Ryu, C.M. (2015). Gaseous 3-pentanol primes plant immunity against a bacterial speck pathogen, *Pseudomonas syringae* pv. tomato via salicylic acid and jasmonic acid-dependent signaling pathways in Arabidopsis. Front. Plant Sci. 6: 821.

Spielmann, F.M., Langebner, S., Ghirardo, A., Hansel, A., Schnitzler, J.P., and Wohlfahrt, G. (2016). Isoprene and α-pinene deposition to grassland mesocosms. Plant and Soil doi: 10.1007/s11104-016-3009-8.

Spoel, S.H., and Dong, X. (2012). How do plants achieve immunity? Defence without specialized immune cells. Nat. Rev. Immunol. 12: 89-100.

Stuttmann, J., Peine, N., Garcia, A.V., Wagner, C., Choudhury, S.R., Wang, Y., James, G.V., Griebel, T., Alcázar, R., Tsuda, K., Schneeberger, K., and Parker, J.E. (2016). Arabidopsis thaliana DM2h (R8) within the Landsberg RPP1-like resistance locus underlies three different cases of EDS1-conditioned autoimmunity. PLoS Genet. 12: e1005990.

Tholl, D., and Lee, S. (2011). Terpene specialized metabolism in *Arabidopsis thaliana*. The Arabidopsis Book 9: e0143.

Truman, W., Bennett, M.H., Kubigsteltig, I., Turnbull, C., and Grant, M. (2007). *Arabidopsis* systemic immunity uses conserved defense signaling pathways and is mediated by jasmonates. Proc. Natl. Acad. Sci. U.S.A. 104: 1075-1080.

Vlot, A.C., Dempsey, D.A., and Klessig, D.F. (2009). Salicylic acid, a multifaceted hormone to combat disease. Annu. Rev. Phytopathol. 47: 177-206.

Wagner, S., Stuttmann, J., Rietz, S., Guerois, R., Brunstein, E., Bautor, J., Niefind, K., and Parker, J.E. (2013). Structural basis for signaling by exclusive EDS1 heteromeric complexes with SAG101 or PAD4 in plant innate immunity. Cell Host Microbe 14: 619-630.

Wang, G., and Dixon, R.A. (2009). Heterodimeric geranyl(geranyl)diphosphate synthase from hop (*Humulus lupulus*) and the evolution of monoterpene biosynthesis. Proc. Natl. Acad. Sci. U.S.A. 106: 9914-9919.

Wang, C., El-Shetehy, M., Shine, M.B., Yu, K., Navarre, D., Wendehenne, D., Kachroo, A., and Kachroo, P. (2014). Free radicals mediate systemic acquired resistance. Cell Rep. 7: 348-355.

Wang, L., Tsuda, K., Sato, M., Cohen, J.D., Katagiri, F., and Glazebrook, J. (2009). Arabidopsis CaM binding protein CBP60g contributes to MAMP-induced SA accumulation and is involved in disease resistance against *Pseudomonas syringae*. PLoS Pathog. 5: e1000301.

Weikl, F., Ghirardo, A., Schnitzler, J.P., and Pritsch, K. (2016). Sesquiterpene emissions from *Alternaria alternata* and *Fusarium oxysporum*: Effects of age, nutrient availability, and co-cultivation. Sci Rep. 6: 22152.

Wickham, H. (2009). ggplot2: elegant graphics for data analysis. Springer, New York.

Wildermuth, M.C., Dewdney, J., Wu, G., and Ausubel, F.M. (2001). Isochorismate synthase is required to synthesize salicylic acid for plant defence. Nature 414: 562-565.

Wittek, F., Kanawati, B., Hoffmann, T., Wenig, M., Franz-Oberdorff, K., Schwab, W., Schmitt-Kopplin, P., and Vlot, A.C. (2015). Folic acid induces salicylic acid-dependent immunity in Arabidopsis and enhances susceptibility to *Alternaria brassicicola*. Mol. Plant Pathol. 16: 616-622.

Wittek, F., Hoffmann, T., Kanawati, B., Bichlmeier, M., Knappe, C., Wenig, M., Schmitt-Kopplin, P., Parker, J.E., Schwab, W., and Vlot, A.C. (2014). Arabidopsis ENHANCED DISEASE SUSCEPTIBILITY1 promotes systemic acquired resistance via azelaic acid and its precursor 9-oxo nonanoic acid. J. Exp. Bot. 65: 5919-5931.

Xia, Y., Gao, Q.M., Yu, K., Lapchyk, L., Navarre, D., Hildebrand, D., Kachroo, A., and Kachroo, P. (2009). An intact cuticle in distal tissues is essential for the induction of systemic acquired resistance in plants. Cell Host Microbe 5: 151-165.

Xiao, Y., Savchenko, T., Baidoo, E.E., Chehab, W.E., Hayden, D.M., Tolstikov, V., Corwin, J.A., Kliebenstein, D.J., Keasling, J.D., and Dehesh, K. (2012). Retrograde signaling by the plastidial metabolite MEcPP regulates expression of nuclear stress-response genes. Cell 149: 1525–1535.

Yi, H.S., Heil, M., Adame-Alvarez, R.M., Ballhorn, D.J., and Ryu, C.M. (2009). Airborne induction and priming of plant defenses against a bacterial pathogen. Plant Physiol. 151: 2152-2161.

Yin, J.L., Wong, W.S., Jang, I.C., and Chua, N.H. (2017). Co-expression of peppermint geranyl diphosphate synthase small subunit enhances monoterpene production in transgenic tobacco plants. New Phytol. 213: 1133-1144.

Yu, K., Soares, J.M., Mandal, M.K., Wang, C., Chanda, B., Gifford, A.N., Fowler, J.S., Navarre, D., Kachroo, A., and Kachroo, P. (2013). A feedback regulatory loop between G3P and lipid transfer proteins DIR1 and AZI1 mediates azelaic-acid-induced systemic immunity. Cell Rep. 3: 1266-1278.

Zoeller, M., Stingl, N., Krischke, M., Fekete, A., Waller, F., Berger, S., and Mueller, M.J. (2012). Lipid profiling of the Arabidopsis hypersensitive response reveals specific lipid peroxidation and fragmentation processes: biogenesis of pimelic and azelaic acid. Plant Physiol. 160: 365-378.

Table 1. Summary of pinene-induced transcriptional changes overlapping with SAR and SA-dependent biological processes (Gene Ontology analysis; *www.arabidopsis.org*). *Q* value (false discovery rate-adjusted *P* value of limma *t*-test) of genes differentially regulated are shown only if <0.05.

Gene	Locus	Full Name	Log_2 Fold Change (LFC)[a]	*P* Value[a]	*Q* Value[a]	Biological Process
PR1	At2g14610	PATHOGENESIS-RELATED GENE 1	2.81	0.011	NA	Systemic acquired resistance, response to water deprivation, response to vitamin B1, defense response
AZI3	At4g12490	AZELEIC ACID INDUCED 3	2.26	0.000	0.025	Defense response to fungus, lipid transport
AZI4	At4g12500	NA	2.19	0.000	0.016	Lipid transport
CHI /AED15	At2g43570	CHITINASE, putative/APOPLASTIC EDS1-DEPENDENT 15	1.97	0.041	NA	Systemic acquired resistance, response to virus, cell wall macromolecule catabolic process, other cellular and metabolic processes
WRKY38	At5g22570	WRKY DNA-BINDING PROTEIN 38	1.88	0.002	NA	Salicylic acid mediated signaling pathway, defense response to bacterium, regulation of transcription
MLO12	At2g39200	MILDEW RESISTANCE LOCUS O 12	1.80	0.000	0.016	Cell death, defense response, defense response to fungus, incompatible interaction, leaf senescence
FRK1	At2g19190	FLG22-INDUCED RECEPTOR-LIKE KINASE 1	1.72	0.000	0.016	Defense response to bacterium, protein phosphorylation
EARLI1	At4g12480	EARLY ARABIDOPSIS ALUMINUM INDUCED 1	1.64	0.000	NA	Induced systemic resistance, defense response to fungus, lipid transport, response to abscisic acid, response to cold, response to salt stress
BBE7	At1g26420	BERBERINE BRIDGE ENZYME 7	1.49	0.000	0.016	Oxidation-reduction process
NA	At3g46280	NA	1.48	0.000	0.018	Phosphorylation
CBP60g	At5g26920	CALMODULIN-BINDING PROTEIN 60G	1.21	0.003	NA	Regulation of systemic acquired resistance, regulation of salicylic acid biosynthetic process, abscisic acid-activated signaling pathway, other cellular and metabolic processes
AZI1	At4g12470	AZELAIC ACID INDUCED 1	0.69	0.008	NA	Systemic acquired resistance, induced systemic resistance, lipid transport, plant-type hypersensitive response, defense response to fungus, other response to cold

[a] Data extracted from Supplemental Dataset 1.

Figure legends

Figure 1 Correlation of VOCs to SAR. The volatile emissions from DEX-treated Col-0 *DEX:AvrRpm1-HA* and *eds1-2 DEX:AvrRpm1-HA* plants were measured by GC-MS and analyzed by orthogonal partial least square regression (OPLS). The left panels (A,C,E) represent sampling period 1 (SP1; VOCs collected 1–4 h after DEX treatment) and the right panels (B,D,F) represent sampling point 2 (SP2; VOCs collected 4–7 h after DEX treatment). A,B) OPLS score plots (green circles, Col-0; red triangles, *eds1-2*). The ellipses indicate the model tolerance based on Hotelling's t^2 with a significance level of a=0.05. Each circle represents an individual measurement of leaf volatiles, given as VOC emission rate (pmol m^{-2} s^{-1}). C,D) OPLS loading plots shown with the correlation scaled. The outer and inner ellipses indicate 100% and 75% of explained variance, respectively. Circles represent the X-loadings (VOCs) and squares depict the Y-loadings (plant genotype). E,F) Correlation coefficient plots of the VOC emission rates correlating VOC emissions with *eds1-2*. The correlation coefficients are scaled and centered, and the error bars are derived from the jack-knife method. Bars represent the average ± standard error of 18–21 replicates. A-F) OPLS model fitness for both the sampling periods (SP1/SP2): r^2 (x) = 61/54 %, q^2 (cum) = 56/34% using 1 predictive component. RMSEE (root mean square error of estimation) =0.35/0.31; RMSEcv (root mean square error of cross validation) = 0.43/0.47; P=0.012/<0.05 cross-validated ANOVA. Significant differences in VOC emissions between Col-0 and *eds1-2* in C–F are highlighted in red (Student's *t*-test, P<0.05,). PC, principal component; α-Pin, α-pinene; β-Pin, β-Pinene; Cam, camphene; Iso, Isopropyl palmitate; Sab, sabinene. Numbers in B–F refer to tentatively identified VOCs (see Supplemental Table 1).

Figure 2 Structures and emission rates of VOCs potentially related to SAR. A) Chemical structures of the VOCs used in this study. Structures were taken or adapted from Chemspider. B–F) Emission rates of α-pinene (B), β-pinene (C), camphene (D), sabinene (E), and isopropyl palmitate (F) from DEX-treated Col-0 *DEX:AvrRpm1-HA* (Col-0) and *eds1-2 DEX:AvrRpm1-HA* (*eds1-2*) plants during sampling period 1 (SP1; 1–4 h after the DEX treatment) and SP2 (4–7 h after the DEX treatment). Emission rates are plotted relative to the projected rosette areas of

the emitting plants. Bars represent the average of 18–21 biologically independent replicates as defined in the Methods ± standard error. Asterisks indicate statistically significant differences from the Col-0 control (Student's *t*-test, P<0.05).

Figure 3 Monoterpene-induced resistance in *A. thaliana* against *Pseudomonas syringae* pathovar *tomato (Pst*). A,C) Plants were exposed as described in the Methods to hexane (negative control; Mock), 1.6 µmole of methyl salicylate (MeSA; positive control), or different concentrations of a mixture (±)α-pinene and (-)β-pinene (1:1 v:v) (Pin; A) or camphene (Cam; C) as indicated below the panels. B) Plants were exposed to hexane (Mock) for 3 d or to 0.6 µmole of Pin for 1, 2, or 3 d followed by 2, 1, or 0 d in the growth chamber (Air) as indicated below the panel. D) Plants were exposed to hexane or to 0.6 µmole of Pin, 0.1 µmole of Cam, or 0.6 µmole of Pin + 0.1 µmole of Cam (Pin + Cam). E,F) Plants were exposed to hexane or to 0.6 µmole of the following pinenes (Pin): (±)α-pinene and (-)β-pinene (1:1 v:v) ((±)α/(-)β), (±)α-pinene and (+)β-pinene (1:1 v:v) ((±)α/(+)β), (±)α-pinene ((±)α), or (-)β-pinene ((-)β) as indicated below the panels. A–F) After 3 d of treatment, the plants were inoculated with *Pst*, and the resulting *in planta Pst* titers were determined at 4 dpi. Bars represent the average of three replicates ± standard deviation, and asterisks (A–C, E) indicate significant differences from the mock controls (Student's *t*-test, P<0.05). Different letters above the bars in (D) indicate statistically significant differences (Student's *t*-test, P<0.05). These experiment were repeated two (B,D) to at least three times (A,C,E,F) with comparable results.

Figure 4 Monoterpene-induced resistance related to SA signaling. Plants were exposed to hexane (negative control; Mock), 1.6 µmole of MeSA (positive control), or 0.6 µmole of (±)α-pinene:(-)β-pinene (1:1 v:v) (Pin) as described in the Methods. A,B) After 3 d, the treated Col-0, *eds1-2*, *npr1-1* (A), and *sid2-1* (B) plants were inoculated with *Pst*, and the resulting *in planta Pst* titers were determined at 4 dpi. Bars represent the average of three replicates ± standard deviation, and asterisks indicate significant differences from the mock controls (Student's *t*-test, P<0.05). (C) After 3 d of treatment, *PR1* transcript accumulation was determined relative to that of *UBIQUITIN* in Col-0 plants by RT-qPCR. Bars represent the average of three

replicates ± standard deviation. These experiments were repeated at least three times with comparable results.

Figure 5 Pinene-triggered changes in the *A. thaliana* gene expression profile. A) Significantly enriched GO terms (TAIR) among the up-regulated genes obtained from microarray data (P<0.05 and $\log_2$ fold change LFC>1). The circle size indicates the number of genes annotated with the respective term. Identical color indicates related GO terms originating from a specific ancestral node. B) Heatmap of all regulated genes (P<0.05 and absolute $\log_2$ fold change |LFC|>1) with consistent direction of change across the four biological replicates. Asterisks indicate genes, whose transcriptional regulation by the pinene mixture was confirmed by RT-qPCR (Supplemental Figure 5).

Figure 6 Monoterpene-induced resistance in Col-0 wt, *azi1-2*, and *gly1-3* mutant plants. The plants were exposed to hexane (negative control/Mock) or to 0.6 µmole of (±)α-pinene:(-)β-pinene (1:1 v:v) (Pin) as described in the Methods. After 3 d, the plants were inoculated with *Pst*, and the resulting *in planta Pst* titers were determined at 4 dpi. Bars represent the average of three replicates ± standard deviation, and asterisks indicate significant differences from the mock controls (Student's *t*-test, P<0.05). This experiment was repeated three times with comparable results.

Figure 7 Superoxide anion radical accumulation in response to pinene treatment. Col-0 wt plants were exposed to hexane (negative control; Mock) or to 0.6 µmole of (±)α-pinene:(-)β-pinene (1:1 v:v) (Pin) as described in the Methods. After 3 d, the accumulation of superoxide anion radicals ($O_2^{\bullet-}$) was visualised with nitroblue tetrazolium (A). The pixel intensity of the pinene-treated leaves was quantified relative to that of the Mock-treated leaves, which was set at 100% (B). Data in (A) and (B) stem from two out of four biologically independent replicate experiments with comparable results. Black bars in (A) indicate 1 cm. Bars in (B) represent the average of 10 replicates ± standard error and asterisks indicate a statistically significant difference from the Mock control (***, Student's *t*-test, P<0.0001).

Figure 8 The prenyltransferase *GERANYLGERANYL REDUCTASE* (*GGR*) is essential for SAR. A) *GGR* transcript accumulation in wt, *ggr1-1*, and *ggr1-2* plants was determined relative to that of *UBIQUITIN* by RT-qPCR. Bars represent the average of three replicates ± standard deviation. B) SAR in wt, *ggr1-1*, and *ggr1-2* plants. Plants were treated in two lower leaves with 10 mM $MgCl_2$ (Mock; M) or with *Pst AvrRpm1* (SAR; S). Three days later, the systemic (2^{nd}) leaves were inoculated with *Pst*, and the resulting *in planta Pst* titers were determined at 4 dpi. C) Monoterpene-induced resistance in wt, *ggr1-1*, and *ggr1-2* plants. Plants were exposed to hexane (negative control; Mock), 1.6 µmole of MeSA (positive control), or 0.6 µmole of (±)α-pinene:(-)β-pinene (1:1 v:v) (Pin) as described in the Methods. After 3 d, the plants were inoculated with *Pst*, and the resulting *in planta Pst* titers were determined at 4 dpi. D) Chemical complementation of the SAR-deficient phenotype of *ggr1-1* plants with pinene. As a primary treatment (1°), Col-0 wt and *ggr1-1* plants were either treated as in (B) in the lanes marked with M and S or left untreated (─). Simultaneously, plants were exposed to hexane (Mock; M) or Pin for 3 d (3d) as in (C) or to Pin for 1 d either on the first (T1), second (T2), or third (T3) d of the normal treatment. Subsequently, all plants were inoculated with *Pst*, and the resulting *in planta Pst* titers were determined at 4 dpi. Bars in B–D represent the average of three replicates ± standard deviation, and asterisks indicate significant differences from the mock controls (Student's *t*-test, $P<0.05$). These experiments were repeated two (A, D) to at least three times (B, C) with comparable results.

Figure 9 Monoterpenes are important for plant-to-plant SAR signaling. Eight wt 'receiver' plants were incubated in gas-tight desiccators together with 12 mock-treated (M) or *Pst AvrRpm1*-infected (S) Col-0 wt, *eds1-2*, or *ggr1-1* 'sender' plants as indicated below the panel. After 3 d, the 'receiver' plants (recipients) were inoculated with *Pst*, and the resulting *in planta Pst* titers were determined at 4 dpi. Bars represent the average of four replicates ± standard deviation, and the asterisk indicates a significant difference from the mock control (Student's *t*-test, $P<0.005$). This experiment was repeated three times with comparable results.

Figure 10 *A. thaliana* monoterpene emissions are induced by *Pst AvrRpm1* and dependent on *GGR.* A-C) Emission rates of α-pinene (A), β-pinene (B), and

camphene (C) from Col-0 wt and *ggr1-1* mutant plants 1 d before (T0) and during the first (T1), second (T2), and third (T3) d after spray inoculation of the plants with *Pst AvrRpm1* or a corresponding mock treatment. VOCs were collected during the day for 8 h per sampling period. Emission rates are plotted relative to the projected rosette areas of the emitting plants. Bars represent the average of 6–7 (Col-0 Mock) to 9 (Col-0 *Pst AvrRpm1*) or 10 (*ggr1-1 Pst AvrRpm1*) biologically independent replicates as defined in the Methods ± standard error. Asterisks indicate statistically significant differences to the corresponding mock controls (Student's *t*-test, P<0.05). ND, not detectable. D) Principal component analysis (PCA) biplot of α-pinene, β-pinene, and camphene emission rates [pmol m^{-2} s^{-1}] from *Pst AvrRpm1*-infected Col-0 (green) and *ggr1-1* (red) plants and from mock-treated Col-0 plants (gray) at T0 (circles), T1 (diamonds), T2 (squares), and T3 (triangles). The ellipses denote 100, 75, and 50% (outer to inner, respectively) explained variance. The arrows were added to indicate the directions of the VOC variables (in black squares) projected into the 2-d plane of the biplot. The variances explained by principal components (PC) 1 and 2 are given in parentheses.

Figure 11 Working model of the role of pinenes in plant immunity. Pinenes accumulate downstream of EDS1 and trigger immunity via EDS1, salicylic acid (SA) biosynthesis (possibly via *CALMODULIN-BINDING PROTEIN 60g* (*CBP60g*)), and NPR1-mediated SA signaling. Also, pinenes trigger the accumulation of superoxide anion radicals ($O_2^{\bullet-}$) that might themselves induce immunity or induce the accumulation of azelaic acid (AzA) promoting SAR together with *AZELAIC ACID INDUCED1* (*AZI1*) and *EARLY ARABIDOPSIS ALUMINIUM INDUCED1* (*EARLI1*). Finally, pinenes induce the expression of *AZI1* and its paralogs *EARLI1*, *AZI3*, and *AZI4*, and act through *AZI1* to enhance immunity. Established interactions are depicted in black and hypothetical interactions are depicted in grey. Solid arrows indicate induction or activation, broken arrows indicate signaling, and the rounded arrows indicate the EDS1-SA positive feedback loop. Proteins are encircled. Genes are in italics and compounds in normal lettering.

Figure 1

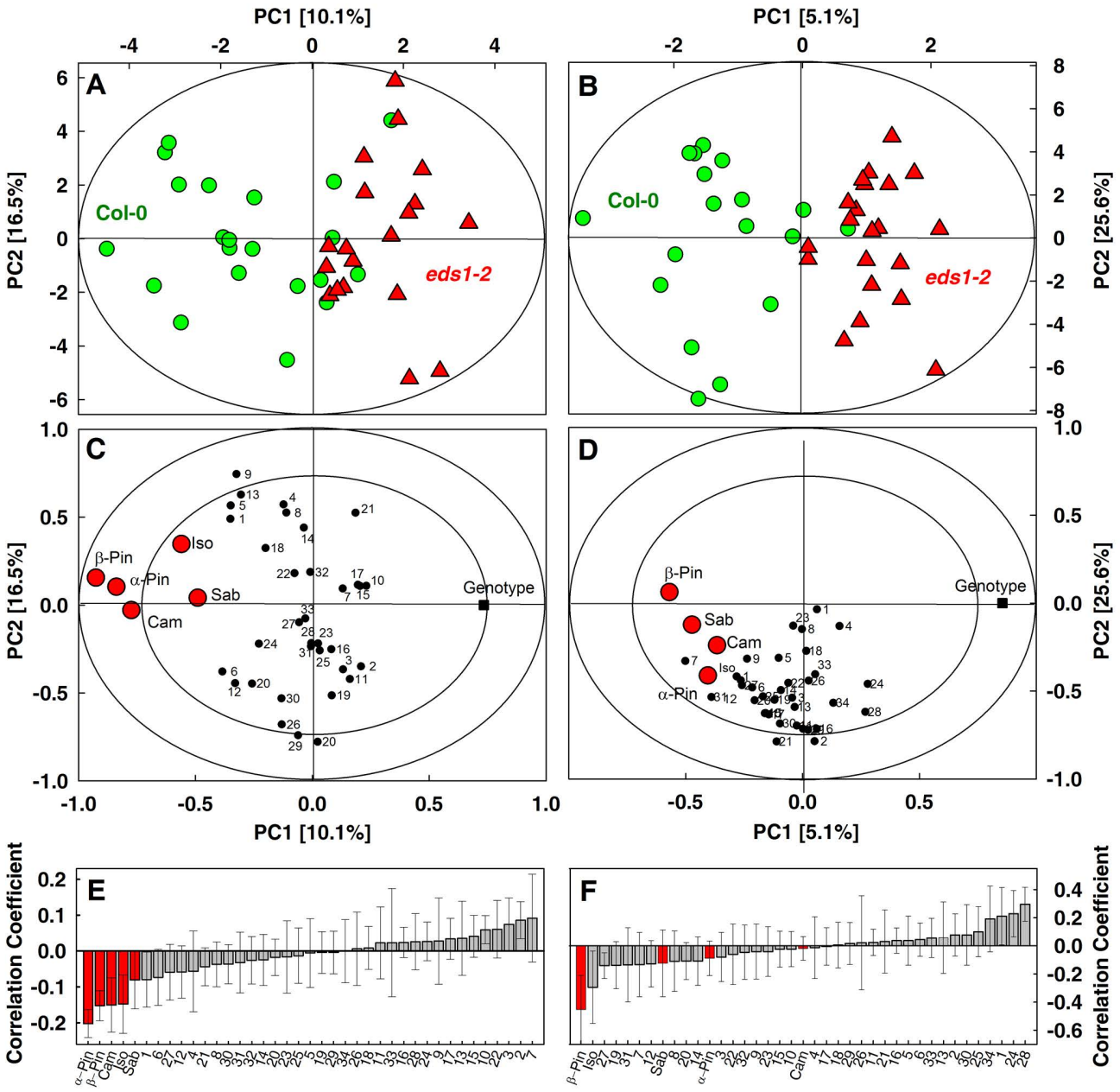
A
B
C
D
E
F
PC1 [10.1%]
PC2 [16.5%]
PC1 [5.1%]
PC2 [25.6%]
Col-0
eds1-2
β-Pin
α-Pin
Iso
Sab
Cam
Genotype
Correlation Coefficient

Figure 1 Correlation of VOCs to SAR. The volatile emissions from DEX-treated Col-0 *DEX:AvrRpm1-HA* and *eds1-2 DEX:AvrRpm1-HA* plants were measured by GC-MS and analyzed by orthogonal partial least square regression (OPLS). The left panels (A,C,E) represent sampling period 1 (SP1; VOCs collected 1–4 h after DEX treatment) and the right panels (B,D,F) represent sampling point 2 (SP2; VOCs collected 4–7 h after DEX treatment). A,B) OPLS score plots (green circles, Col-0; red triangles, *eds1-2*). The ellipses indicate the model tolerance based on Hotelling's t^2 with a significance level of a=0.05. Each circle represents an individual measurement of leaf volatiles, given as VOC emission rate (pmol m^{-2} s^{-1}). C,D) OPLS loading plots shown with the correlation scaled. The outer and inner ellipses indicate 100% and 75% of explained variance, respectively. Circles represent the X-loadings (VOCs) and squares depict the Y-loadings (plant genotype). E,F) Correlation coefficient plots of the VOC emission rates correlating VOC emissions with *eds1-2*. The correlation coefficients are scaled and centered, and the error bars are derived from the jack-knife method. Bars represent the average ± standard error of 18–21 replicates. A-F) OPLS model fitness for both the sampling periods (SP1/SP2): r^2 (x) = 61/54 %, q^2 (cum) = 56/34% using 1 predictive component. RMSEE (root mean square error of estimation) =0.35/0.31; RMSEcv (root mean square error of cross validation) = 0.43/0.47; P=0.012/<0.05 cross-validated ANOVA. Significant differences in VOC emissions between Col-0 and *eds1-2* in C–F are highlighted in red (Student's *t*-test, P<0.05,). PC, principal component; α-Pin, α-pinene; β-Pin, β-Pinene; Cam, camphene; Iso, Isopropyl palmitate; Sab, sabinene. Numbers in B–F refer to tentatively identified VOCs (see Supplemental Table 1).

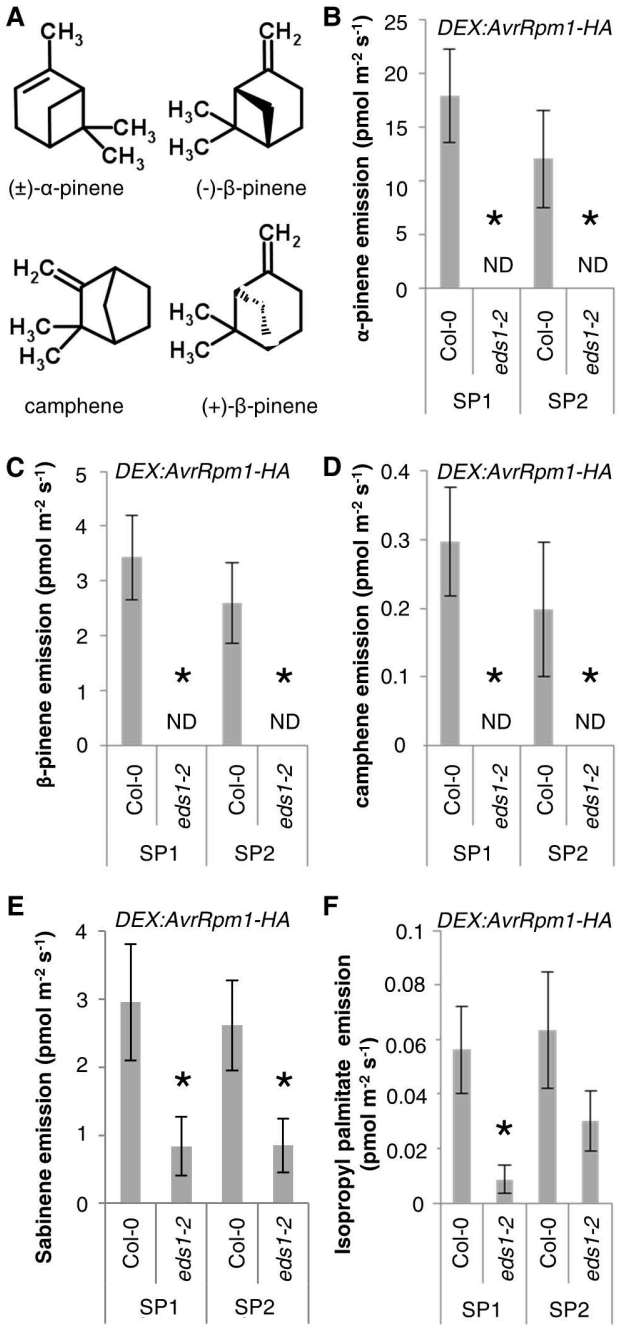

Figure 2 Structures and emission rates of VOCs potentially related to SAR. A) Chemical structures of the VOCs used in this study. Structures were taken or adapted from Chemspider. B–F) Emission rates of α-pinene (B), β-pinene (C), camphene (D), sabinene (E), and isopropyl palmitate (F) from DEX-treated Col-0 *DEX:AvrRpm1-HA* (Col-0) and *eds1-2 DEX:AvrRpm1-HA* (*eds1-2*) plants during sampling period 1 (SP1; 1–4 h after the DEX treatment) and SP2 (4–7 h after the DEX treatment). Emission rates are plotted relative to the projected rosette areas of the emitting plants. Bars represent the average of 18–21 biologically independent replicates as defined in the Methods ± standard error. Asterisks indicate statistically significant differences from the Col-0 control (Student's *t*-test , P<0.05).

Figure 3

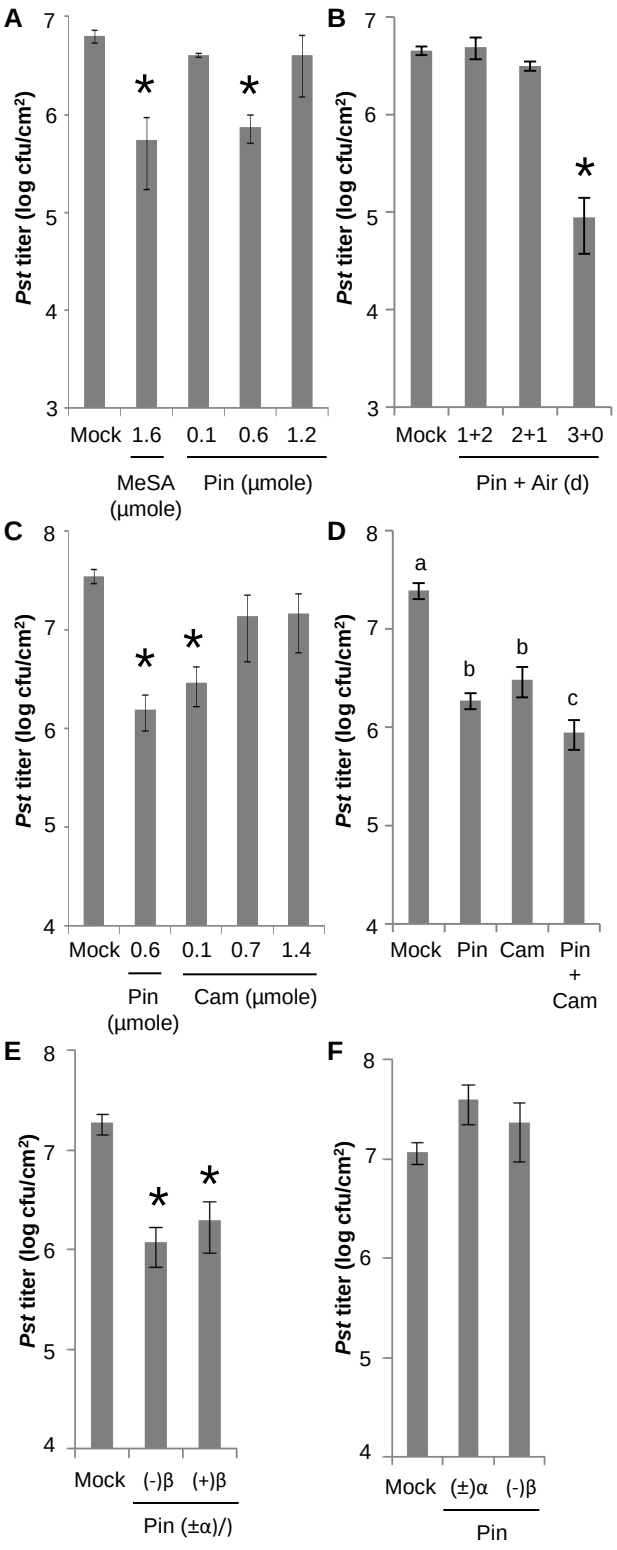
A
B
C
D
E
F
Pst titer (log cfu/cm²)
Mock
1.6
0.1
0.6
1.2
MeSA (µmole)
Pin (µmole)
1+2
2+1
3+0
Pin + Air (d)
0.7
1.4
Cam (µmole)
Pin
Cam
Pin + Cam
(-)β
(+)β
Pin (±α)/)
(±)α
a
b
c

Figure 3 Monoterpene-induced resistance in *A. thaliana* against *Pseudomonas syringae* pathovar *tomato (Pst*). A,C) Plants were exposed as described in the Methods to hexane (negative control; Mock), 1.6 µmole of methyl salicylate (MeSA; positive control), or different concentrations of a mixture (±)α-pinene and (-)β-pinene (1:1 v:v) (Pin; A) or camphene (Cam; C) as indicated below the panels. B) Plants were exposed to hexane (Mock) for 3 d or to 0.6 µmole of Pin for 1, 2, or 3 d followed by 2, 1, or 0 d in the growth chamber (Air) as indicated below the panel. D) Plants were exposed to hexane or to 0.6 µmole of Pin, 0.1 µmole of Cam, or 0.6 µmole of Pin + 0.1 µmole of Cam (Pin + Cam). E,F) Plants were exposed to hexane or to 0.6 µmole of the following pinenes (Pin): (±)α-pinene and (-)β-pinene (1:1 v:v) ((±)α/(-)β), (±)α-pinene and (+)β-pinene (1:1 v:v) ((±)α/(+)β), (±)α-pinene ((±)α), or (-)β-pinene ((-)β) as indicated below the panels. A–F) After 3 d of treatment, the plants were inoculated with *Pst*, and the resulting *in planta Pst* titers were determined at 4 dpi. Bars represent the average of three replicates ± standard deviation, and asterisks (A–C, E) indicate significant differences from the mock controls (Student's *t*-test, $P<0.05$). Different letters above the bars in (D) indicate statistically significant differences (Student's *t*-test, $P<0.05$). These experiment were repeated two (B,D) to at least three times (A,C,E,F) with comparable results.

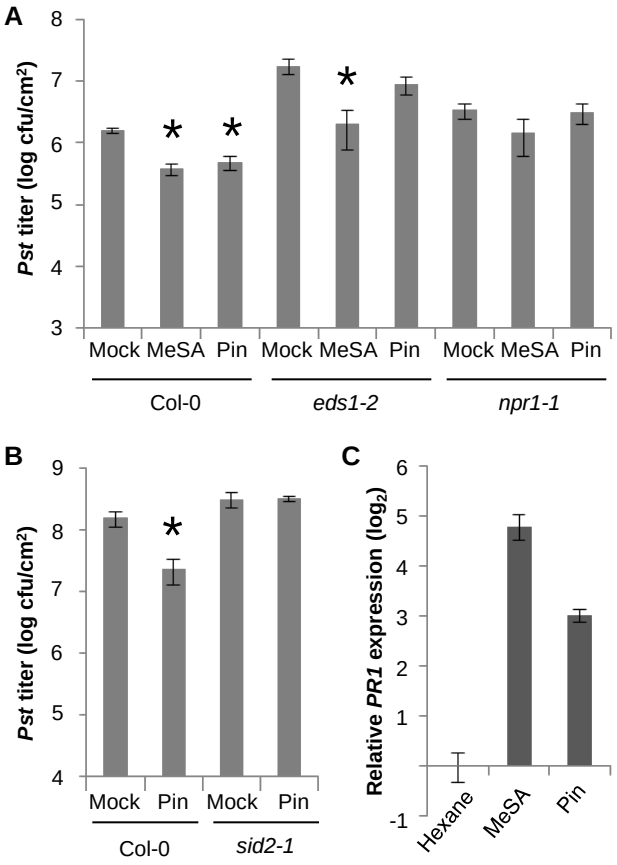

Figure 4 Monoterpene-induced resistance related to SA signaling. Plants were exposed to hexane (negative control; Mock), 1.6 µmole of MeSA (positive control), or 0.6 µmole of (±)α-pinene:(-)β-pinene (1:1 v:v) (Pin) as described in the Methods. A,B) After 3 d, the treated Col-0, *eds1-2*, *npr1-1* (A), and *sid2-1* (B) plants were inoculated with *Pst*, and the resulting *in planta Pst* titers were determined at 4 dpi. Bars represent the average of three replicates ± standard deviation, and asterisks indicate significant differences from the mock controls (Student's *t*-test, P<0.05). (C) After 3 d of treatment, *PR1* transcript accumulation was determined relative to that of *UBIQUITIN* in Col-0 plants by RT-qPCR. Bars represent the average of three replicates ± standard deviation. These experiments were repeated at least three times with comparable results.

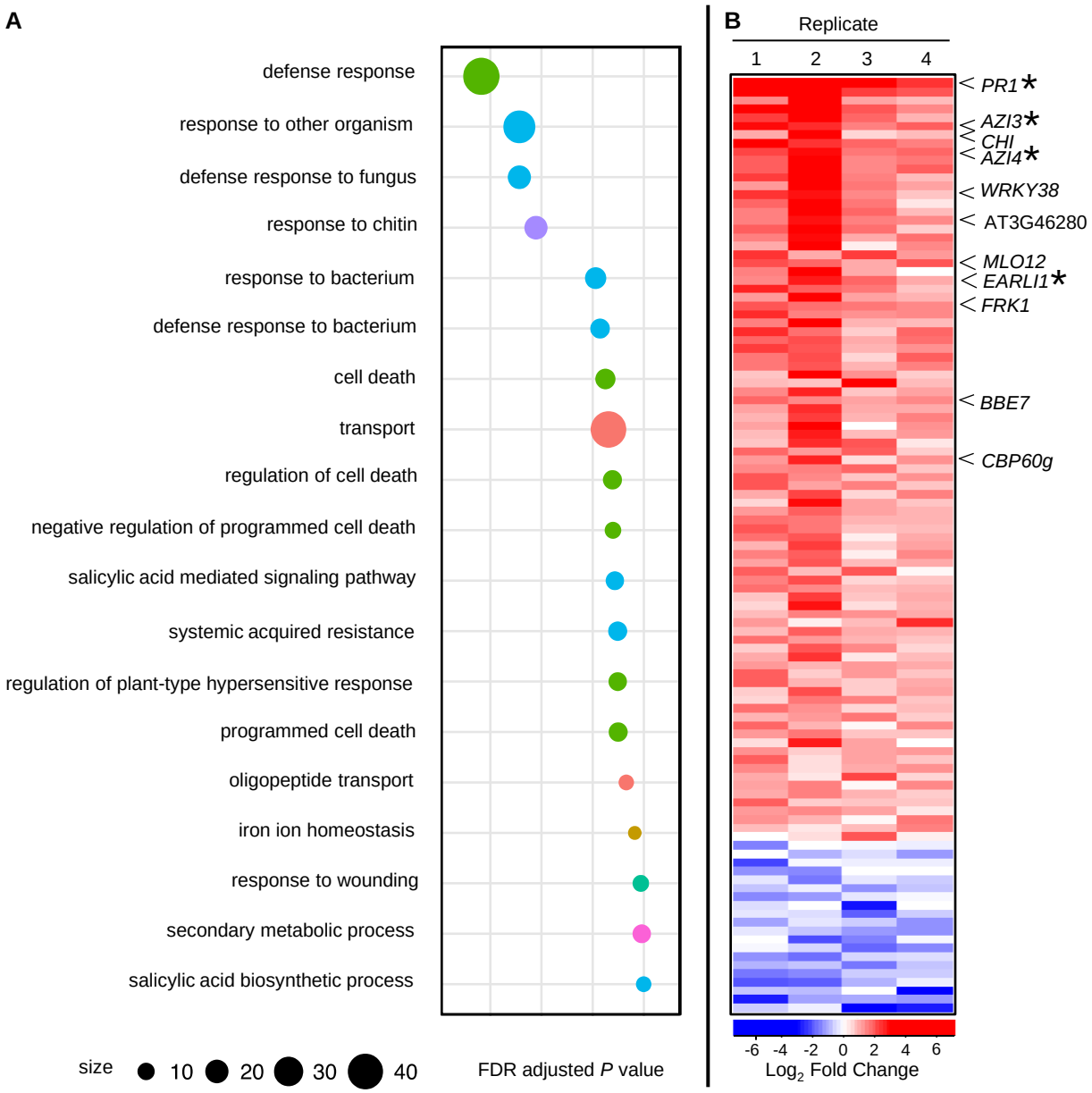

Figure 5 Pinene-triggered changes in the *A. thaliana* gene expression profile. A) Significantly enriched GO terms (TAIR) among the up-regulated genes obtained from microarray data (P<0.05 and $\log_2$ fold change LFC>1). The circle size indicates the number of genes annotated with the respective term. Identical color indicates related GO terms originating from a specific ancestral node. B) Heatmap of all regulated genes (P<0.05 and absolute $\log_2$ fold change |LFC|>1) with consistent direction of change across the four biological replicates. Asterisks indicate genes, whose transcriptional regulation by the pinene mixture was confirmed by RT-qPCR (Supplemental Figure 5).

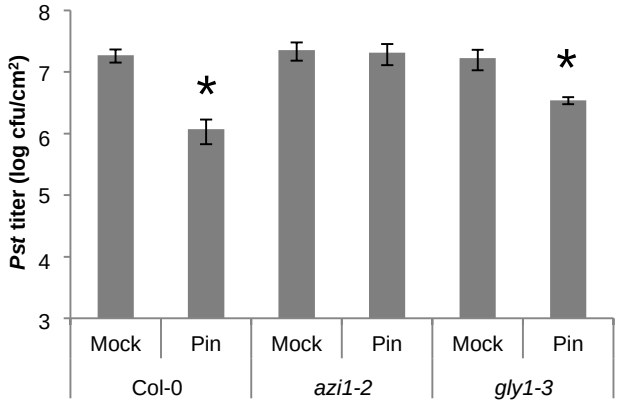

Figure 6 Monoterpene-induced resistance in Col-0 wt, *azi1-2*, and *gly1-3* mutant plants. The plants were exposed to hexane (negative control/Mock) or to 0.6 µmole of (±)α-pinene:(-)β-pinene (1:1 v:v) (Pin) as described in the Methods. After 3 d, the plants were inoculated with *Pst*, and the resulting *in planta Pst* titers were determined at 4 dpi. Bars represent the average of three replicates ± standard deviation, and asterisks indicate significant differences from the mock controls (Student's *t*-test, $P<0.05$). This experiment was repeated three times with comparable results.

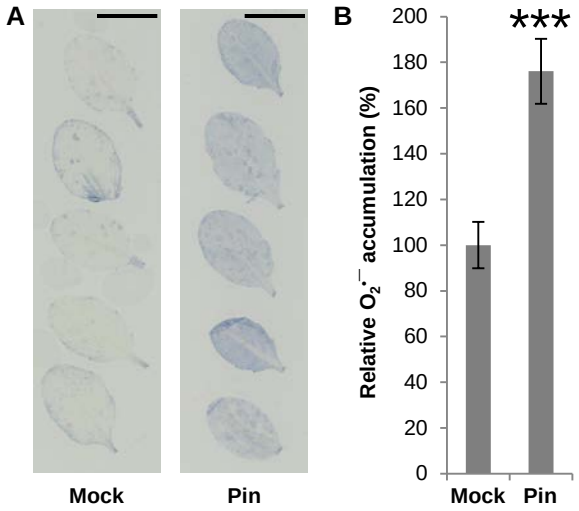

Figure 7 Superoxide anion radical accumulation in response to pinene treatment. Col-0 wt plants were exposed to hexane (negative control; Mock) or to 0.6 µmole of (±)α-pinene:(-)β-pinene (1:1 v:v) (Pin) as described in the Methods. After 3 d, the accumulation of superoxide anion radicals ($O_2^{\bullet-}$) was visualised with nitroblue tetrazolium (A). The pixel intensity of the pinene-treated leaves was quantified relative to that of the Mock-treated leaves, which was set at 100% (B). Data in (A) and (B) stem from two out of four biologically independent replicate experiments with comparable results. Black bars in (A) indicate 1 cm. Bars in (B) represent the average of 10 replicates ± standard error and asterisks indicate a statistically significant difference from the Mock control (***, Student's *t*-test, P<0.0001).

Figure 8

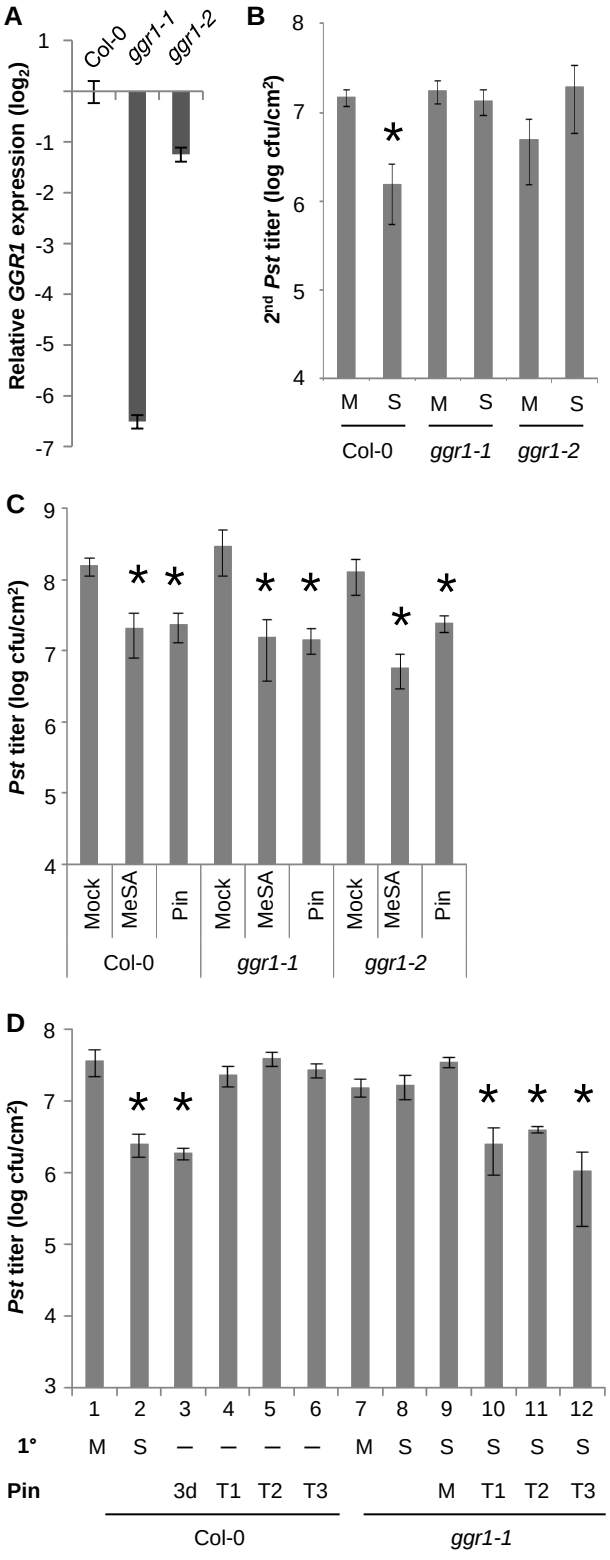
A
Relative GGR1 expression (log2)
Col-0
ggr1-1
ggr1-2
B
2nd Pst titer (log cfu/cm2)
M S M S M S
Col-0 ggr1-1 ggr1-2
C
Pst titer (log cfu/cm2)
Mock MeSA Pin Mock MeSA Pin Mock MeSA Pin
Col-0 ggr1-1 ggr1-2
D
Pst titer (log cfu/cm2)
1 2 3 4 5 6 7 8 9 10 11 12
1° M S – – – – M S S S S S
Pin 3d T1 T2 T3 M T1 T2 T3
Col-0 ggr1-1

Figure 8 The prenyltransferase *GERANYLGERANYL REDUCTASE* (*GGR*) is essential for SAR. A) *GGR* transcript accumulation in wt, *ggr1-1*, and *ggr1-2* plants was determined relative to that of *UBIQUITIN* by RT-qPCR. Bars represent the average of three replicates ± standard deviation. B) SAR in wt, *ggr1-1*, and *ggr1-2* plants. Plants were treated in two lower leaves with 10 mM $MgCl_2$ (Mock; M) or with *Pst AvrRpm1* (SAR; S). Three days later, the systemic (2^{nd}) leaves were inoculated with *Pst*, and the resulting *in planta Pst* titers were determined at 4 dpi. C) Monoterpene-induced resistance in wt, *ggr1-1*, and *ggr1-2* plants. Plants were exposed to hexane (negative control; Mock), 1.6 µmole of MeSA (positive control), or 0.6 µmole of (±)α-pinene:(-)β-pinene (1:1 v:v) (Pin) as described in the Methods. After 3 d, the plants were inoculated with *Pst*, and the resulting *in planta Pst* titers were determined at 4 dpi. D) Chemical complementation of the SAR-deficient phenotype of *ggr1-1* plants with pinene. As a primary treatment (1°), Col-0 wt and *ggr1-1* plants were either treated as in (B) in the lanes marked with M and S or left untreated (–). Simultaneously, plants were exposed to hexane (Mock; M) or Pin for 3 d (3d) as in (C) or to Pin for 1 d either on the first (T1), second (T2), or third (T3) d of the normal treatment. Subsequently, all plants were inoculated with *Pst*, and the resulting *in planta Pst* titers were determined at 4 dpi. Bars in B–D represent the average of three replicates ± standard deviation, and asterisks indicate significant differences from the mock controls (Student's *t*-test, $P<0.05$). These experiments were repeated two (A, D) to at least three times (B, C) with comparable results.

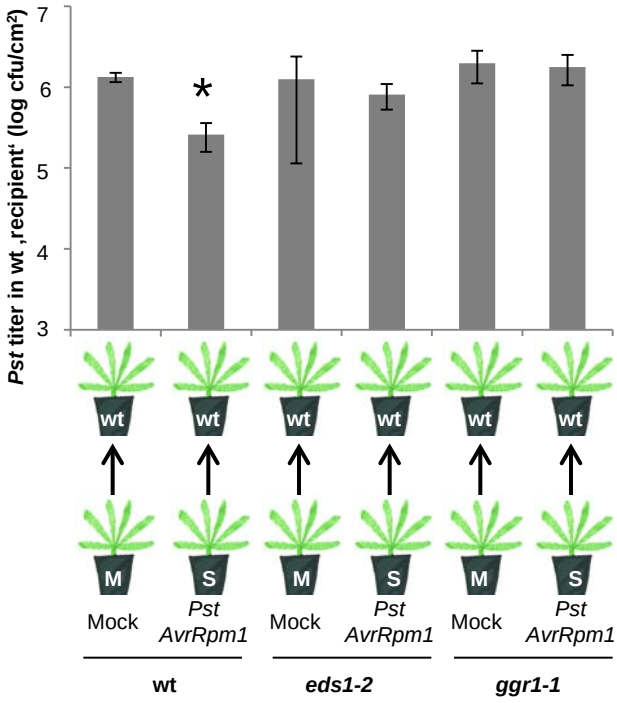

Figure 9 Monoterpenes are important for plant-to-plant SAR signaling. Eight wt 'receiver' plants were incubated in gas-tight desiccators together with 12 mock-treated (M) or *Pst AvrRpm1*-infected (S) Col-0 wt, *eds1-2*, or *ggr1-1* 'sender' plants as indicated below the panel. After 3 d, the 'receiver' plants (recipients) were inoculated with *Pst*, and the resulting *in planta Pst* titers were determined at 4 dpi. Bars represent the average of four replicates ± standard deviation, and the asterisk indicates a significant difference from the mock control (Student's *t*-test, P<0.005). This experiment was repeated three times with comparable results.

Figure 10

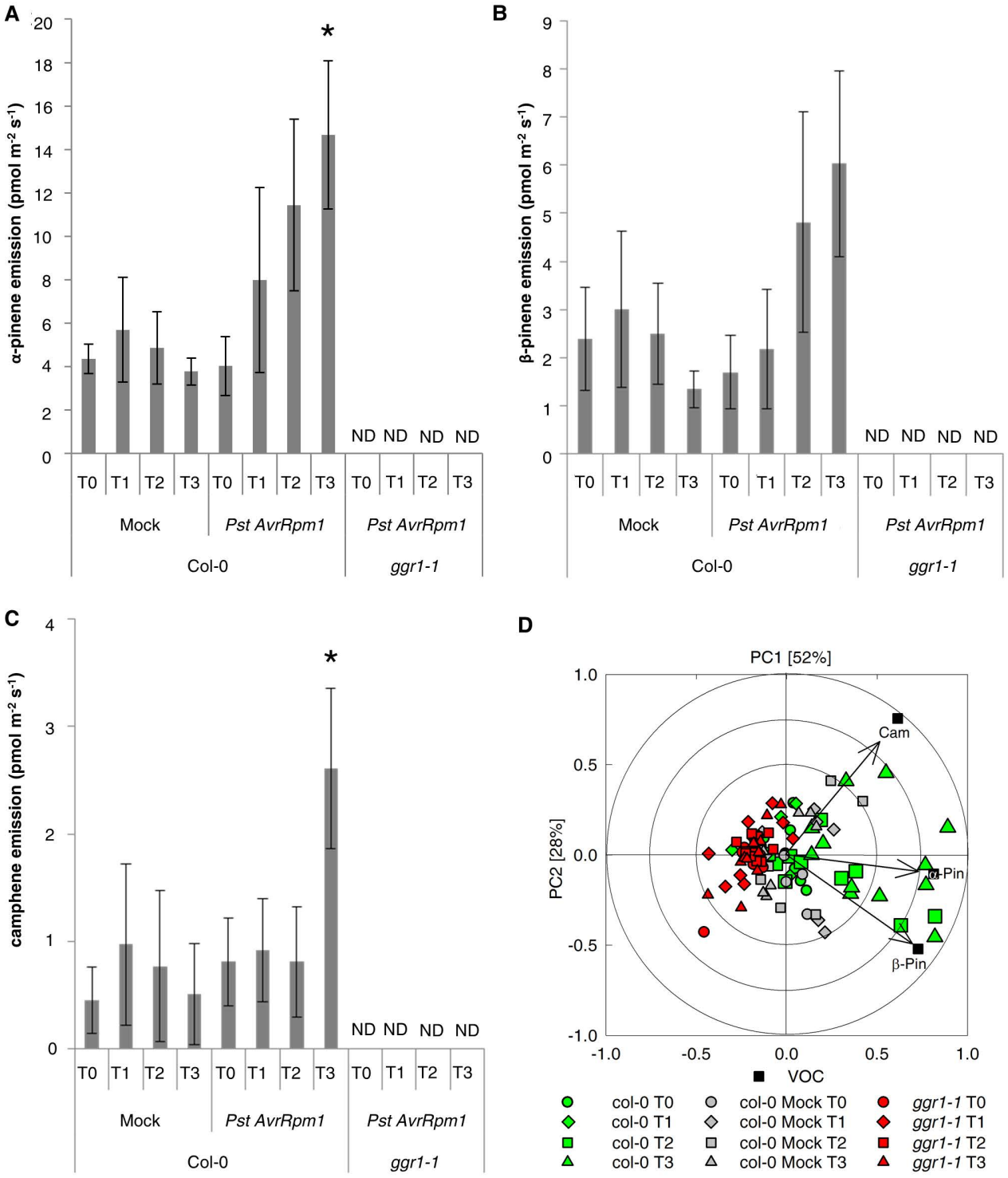
A
α-pinene emission (pmol m-2 s-1)
20
18
16
14
12
10
8
6
4
2
0
*
ND ND ND ND
T0 T1 T2 T3 T0 T1 T2 T3 T0 T1 T2 T3
Mock
Pst AvrRpm1
Pst AvrRpm1
Col-0
ggr1-1
B
β-pinene emission (pmol m-2 s-1)
9
8
7
6
5
4
3
2
1
0
ND ND ND ND
T0 T1 T2 T3 T0 T1 T2 T3 T0 T1 T2 T3
Mock
Pst AvrRpm1
Pst AvrRpm1
Col-0
ggr1-1
C
camphene emission (pmol m-2 s-1)
4
3
2
1
0
*
ND ND ND ND
T0 T1 T2 T3 T0 T1 T2 T3 T0 T1 T2 T3
Mock
Pst AvrRpm1
Pst AvrRpm1
Col-0
ggr1-1
D
PC1 [52%]
PC2 [28%]
1.0
0.5
0.0
-0.5
-1.0
-1.0 -0.5 0.0 0.5 1.0
VOC
Cam
α-Pin
β-Pin
col-0 T0
col-0 T1
col-0 T2
col-0 T3
col-0 Mock T0
col-0 Mock T1
col-0 Mock T2
col-0 Mock T3
ggr1-1 T0
ggr1-1 T1
ggr1-1 T2
ggr1-1 T3

Figure 10 *A. thaliana* monoterpene emissions are induced by *Pst AvrRpm1* and dependent on *GGR.* A-C) Emission rates of α-pinene (A), β-pinene (B), and camphene (C) from Col-0 wt and *ggr1-1* mutant plants 1 d before (T0) and during the first (T1), second (T2), and third (T3) d after spray inoculation of the plants with *Pst AvrRpm1* or a corresponding mock treatment. VOCs were collected during the day for 8 h per sampling period. Emission rates are plotted relative to the projected rosette areas of the emitting plants. Bars represent the average of 6–7 (Col-0 Mock) to 9 (Col-0 *Pst AvrRpm1*) or 10 (*ggr1-1 Pst AvrRpm1*) biologically independent replicates as defined in the Methods ± standard error. Asterisks indicate statistically significant differences to the corresponding mock controls (Student's *t*-test , $P<0.05$). ND, not detectable. D) Principal component analysis (PCA) biplot of α-pinene, β-pinene, and camphene emission rates [pmol m^{-2} s^{-1}] from *Pst AvrRpm1*-infected Col-0 (green) and *ggr1-1* (red) plants and from mock-treated Col-0 plants (gray) at T0 (circles), T1 (diamonds), T2 (squares), and T3 (triangles). The ellipses denote 100, 75, and 50% (outer to inner, respectively) explained variance. The arrows were added to indicate the directions of the VOC variables (in black squares) projected into the 2-d plane of the biplot. The variances explained by principal components (PC) 1 and 2 are given in parentheses.

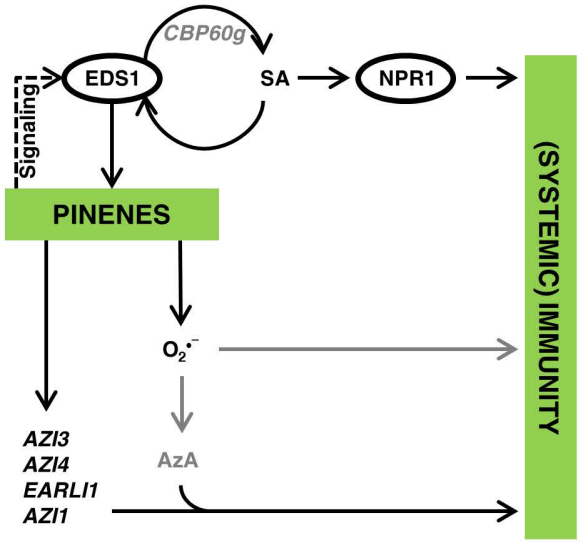

Figure 11 Working model of the role of pinenes in plant immunity. Pinenes accumulate downstream of EDS1 and trigger immunity via EDS1, salicylic acid (SA) biosynthesis (possibly via *CALMODULIN-BINDING PROTEIN 60g* (*CBP60g*)), and NPR1-mediated SA signaling. Also, pinenes trigger the accumulation of superoxide anion radicals ($O_2^{\bullet-}$) that might themselves induce immunity or induce the accumulation of azelaic acid (AzA) promoting SAR together with *AZELAIC ACID INDUCED1* (*AZI1*) and *EARLY ARABIDOPSIS ALUMINIUM INDUCED1* (*EARLI1*). Finally, pinenes induce the expression of *AZI1* and its paralogs *EARLI1*, *AZI3*, and *AZI4*, and act through *AZI1* to enhance immunity. Established interactions are depicted in black and hypothetical interactions are depicted in grey. Solid arrows indicate induction or activation, broken arrows indicate signaling, and the rounded arrows indicate the EDS1-SA positive feedback loop. Proteins are encircled. Genes are in italics and compounds in normal lettering.